

Supporting Information

Long-term sciatic nerve block lead by supramolecular arrangement of self-delivery local anesthetic nano systems

Lei Tang,^{*a,b} Feng Qin,^c Deying Gong,^{a,b} Yu Dong,^d LiLi Pan,^c Changcui Zhou,^{a,b} Qinqin Yin,^a Xinghai Song,^{a,b} Rui Ling,^{a,b} Junlong Huang,^{a,b} Qin Fan,^c Wenhao Yi,^c Fengbo Wu,^c Xiaoi Wu,^c Weiyi Zhang,^a Jun Yang^{*a,b} and Ji-Yu Wang^{*c}

- Department of Anesthesiology, West China Hospital, Sichuan University, Chengdu 610041, P.R. China.
- Laboratory of Anesthesia and Critical Care Medicine, National-Local Joint Engineering Research Centre of Translational Medicine of Anesthesiology, West China Hospital, Sichuan University, Chengdu 610041, P.R. China.
- West China Hospital, Sichuan University, Chengdu 610041, P.R. China.
- College of Chemistry and Life Science, Sichuan Provincial Key Laboratory for Structural Optimization and Application of Functional Molecules, Chengdu Normal University, Chengdu, 611130, P.R. China.
- Department of Chemistry, Xihua University, Chengdu, P.R. China.

Corresponding Author:

Lei Tang: manstein_1984@sina.com

Jun Yang: yang215jun@163.com

Ji-Yu Wang: jiyuwang@cioc.ac.cn

Claim:

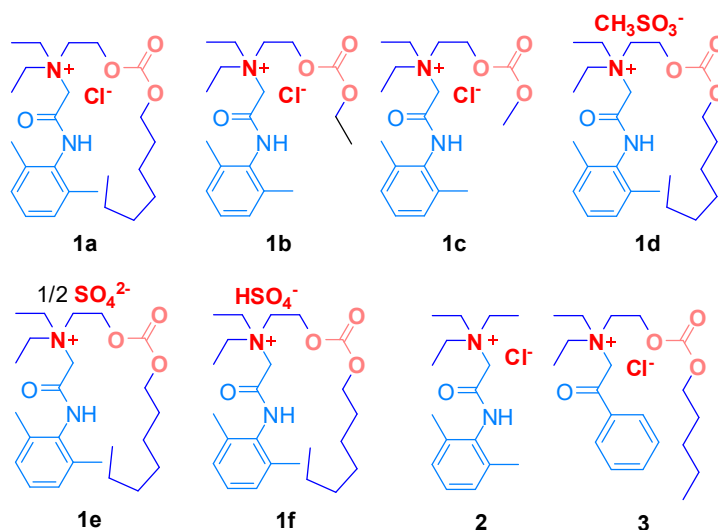
The animal experiments were performed in accordance with the guide for the care and use of medical laboratory animals (Ministry of Health, China). All animal procedures in this work were approved by the Institutional Animal Experimental Ethics Committee of Sichuan University (Chengdu, China, 13 Approval file No. 2015014A).

Table of Contents

SI.1 Synthesis and structure information	P2
SI.2 TEM observation	P9
SI.3 2D-NMR analysis	P11
SI.4 Surface tension and CMC measurement	P33
SI.5 Plasma decomposition measurement	P39
SI.6 Rats' sensory block and neuropathological injury measurement	P41
SI.7 Slow release on local tissue measurement	P45
SI.8 <i>in vitro</i> diffusion determination on sciatic nerve	P47
SI.9 Data summary	P48
Reference	P50

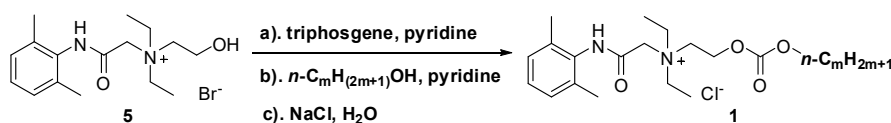
SI.1 Synthesis and structure information

Small organic surfactant used in this work were shown in Scheme S1 :



Scheme S1 Chemical structure of surfactant

Specific operation and results



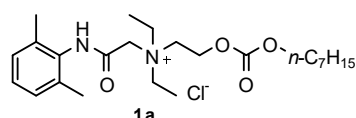
General method on synthesis of product 1

To the mixture of **5** (6.0g, 16.7 mmol), triphosgene (2.47 g, 8.34 mmol) and 1,2-dichloroethane

(60 mL), pyridine (1.4 g, 17.6 mmol) in 1,2-dichloroethane (20 mL) were added dropwise at room temperature for 20min. After addition, this mixture was allowed to stirring at 50°C for 2h. Then the fatty alcohol (16.7 mmol) in 1,2-dichloroethane (30 mL) was added. This solution was stirred for another 16h at 50°C, and cooled to room temperature.

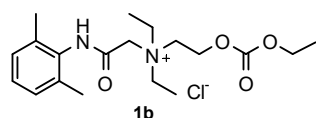
Saturated brine (30 mL) was poured into the reaction flask. The organic layer was washed with saturated brine (20 mL x 7). The organic solvent was removed in vacuo. The residue was further purified by chromatography with CH₂Cl₂-CH₃OH to give product (1) as white powder.

Characterization data of compounds 1^{SI}



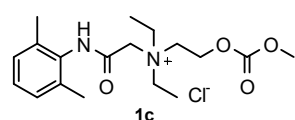
2-(2,6-dimethylphenylamino)-N,N-diethyl-N-(2-(heptyloxy)ethyl)-2-oxoethanaminium chloride (1a). Obtained

as white powder, yield: 36%. Melting Point: 136.7~138.6°C. ¹H NMR (400 MHz, CDCl₃)δ: 10.34 (s, 1H), 7.00~7.08 (m, 3H), 5.00 (m, 2H), 4.64 (br, 2H), 4.16 (t, *J* = 6.8 Hz, 2H), 4.04 (m, 2H), 3.66~3.76 (m, 4H), 2.24 (s, 6H), 1.60~1.63 (m, 2H), 1.54~1.56 (m, 8H), 0.86 (t, *J* = 7.2 Hz, 3H). ¹³C NMR (100 MHz, CDCl₃)δ: 8.33, 14.06, 14.19, 18.82, 21.06, 22.54, 25.53, 26.89, 28.48, 28.81, 31.64, 56.40, 57.56, 57.82, 60.39, 60.59, 69.33, 76.79, 127.42, 128.12, 133.11, 135.04, 154.31, 161.77. HRMS: [C₂₄H₄₁N₂O₄]⁺: 421.3107, found: 421.3070. Content of Cl⁻ by IC: 99.0%.



2-(2,6-dimethylphenylamino)-N,N-diethyl-N-(2-(ethoxycarbonyloxy)ethyl)-N,N-diethyl-2-oxoethanaminium chloride (1b) Obtained as

white powder, yield: 43%. Melting Point: 157.7~158.5°C. ¹H NMR (400 MHz, CDCl₃)δ: 10.48 (s, 1H), 7.04~7.11 (m, 3H), 5.05 (br, 2H), 4.68 (br, 2H), 4.22 (t, *J* = 7.1 Hz, 2H), 4.06 (br, 2H), 3.74 (br, 2H), 2.27 (br, 6H), 1.52 (br, 6H), 1.30 (t, *J* = 7.1 Hz, 3H). ¹³C NMR (100 MHz, CDCl₃)δ: 8.52, 14.16, 18.90, 56.59, 57.88, 60.64, 65.08, 127.57, 128.17, 132.88, 135.12, 154.15, 161.79. HRMS: [C₁₉H₃₁N₂O₄]⁺: 351.2778, found: 351.2650. Content of Cl⁻: 98.9%.



2-(2,6-dimethylphenylamino)-N,N-diethyl-N-(2-(methoxycarbonyloxy)ethyl)-2-oxoethanaminium chloride (1c) Obtained as white

powder, yield: 22%. Melting Point: 136.2~137.6°C. ¹H NMR (400 MHz, CDCl₃)δ: 10.65 (s, 1H), 7.00~7.04 (m, 3H), 4.96 (s, 2H), 4.61 (s, 2H), 4.02 (s, 2H), 3.75 (s, 3H), 3.68 (m, 4H), 2.22 (s, 6H), 1.45 (s, 6H). ¹³C NMR (100 MHz, CDCl₃)δ: 8.23, 18.81, 55.46, 56.41, 57.61, 57.73, 60.86, 127.49, 128.12, 132.90, 135.05, 154.69, 161.75. HRMS: [C₁₈H₂₉N₂O₄]⁺: 337.2122, found: 337.2118. Content of Cl⁻: 99.0%.

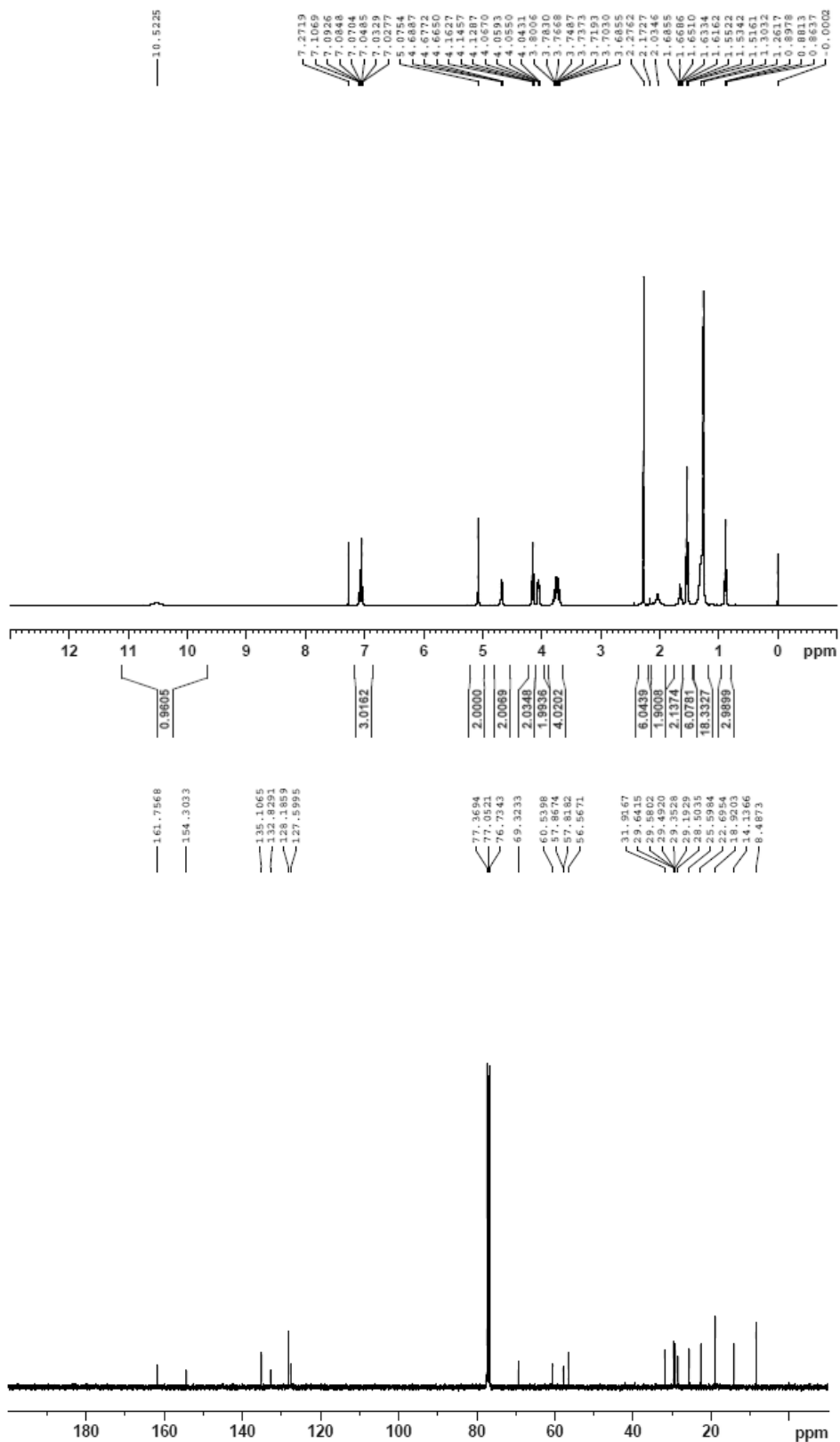


Figure S1 ^1H NMR, ^{13}C NMR of compound 1b

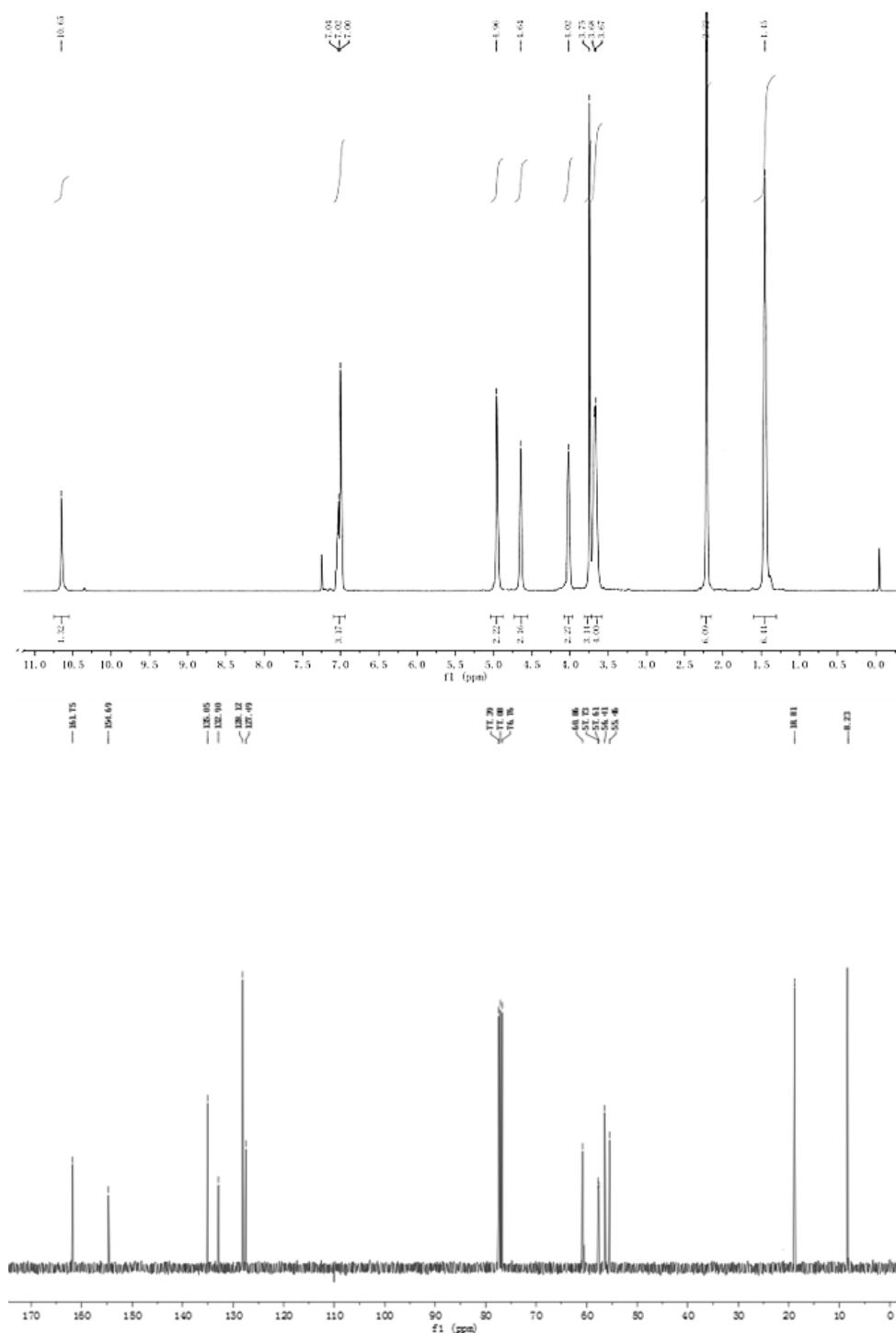
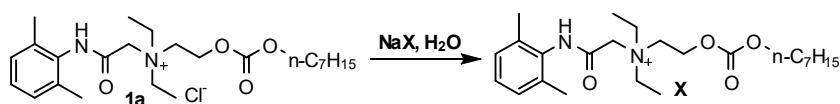


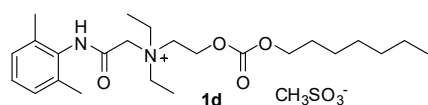
Figure S2 ^1H NMR, ^{13}C NMR of compound **1c**



Method on synthesis of product **1d~1f**

Compound **1a** (20.0g) was dissolved in CH_2Cl_2 (300mL). Saturated solution of NaX ($\text{X} = \text{CH}_3\text{SO}_3^-$, $1/2\text{SO}_4^{2-}$ or HSO_4^-) 10mL was added. The organic layer was washed with saturated

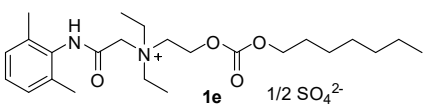
solution of NaX (10 mL x 10). The organic solvent was removed in vacuo. The residue was further purified by chromatography with CH₂Cl₂-CH₃OH as eluent to give product (1d~1f).



2-(2,6-dimethylphenylamino)-N,N-diethyl-N-(2-(heptyloxycarbonyloxy)ethyl)-2-oxoethanaminium

methane sulfonate (1d) Obtained as colorless syrups,

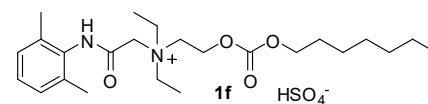
yield: 48%. ¹H NMR (300 MHz, d₆-DMSO) δ: 10.05 (s, 1H), 7.08~7.12 (m, 3H), 4.56~4.58 (m, 2H), 4.42 (s, 2H), 4.07~4.10 (m, 2H), 3.97~3.99 (m, 2H), 3.61~3.67 (m, 2H), 2.31 (s, 3H), 2.17 (s, 6H), 1.56~1.58 (m, 2H), 1.33~1.24 (m, 14H), 0.86 (t, *J* = 7.2 Hz, 3H).



2-(2,6-dimethylphenylamino)-N,N-diethyl-N-(2-(heptyloxycarbonyloxy)ethyl)-2-oxoethanaminium sulfate

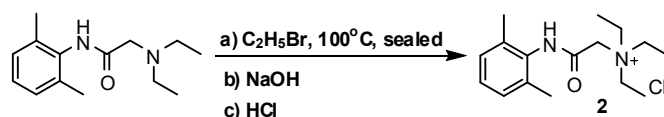
(1e) Obtained as slight yellow syrups, yield: 9%. Content

of SO₄²⁻ in whole compound: 11.6% (Content of counter ion in calculated amount: 10.23% for SO₄²⁻ and 18.55% for HSO₄⁻. Actual ratio of SO₄²⁻ : HSO₄⁻ was 2.8 : 1).



2-(2,6-dimethylphenylamino)-N,N-diethyl-N-(2-(heptyloxycarbonyloxy)ethyl)-2-oxoethanaminium

hydrogensulfate (1f) Obtained as slight yellow syrups, yield: 7%. Content of HSO₄⁻: 92.4%.



Lidocaine 10 g and bromoethane 30 mL were added in a flask, sealed and heated at 100 °C for 10 hours. The reaction residual was cooled to room temperature, added with ethyl acetate 30mL and filtered. After washed with ethyl acetate (20mL x 2), the solid residue as white powder was dissolved in CH₂Cl₂ 200mL. The organic layer was washed with water solution of NaOH (40%, 10 mL x 5) and evaporated under vacuo to give product as light yellow powder.

This light yellow powder was dissolved in CH₂Cl₂ 200mL, and mixed with HCl at 0°C with vigorous stirring. The organic solvent was removed. The residue was purified by chromatography with CH₂Cl₂-CH₃OH as eluent to give product **2** as white solid, yield: 13%. Melting Point: 165.4~166.3°C. ¹H NMR (400 MHz, CDCl₃)δ: 6.97~7.04 (m, 3H), 4.72 (br, 2H), 3.57 (q, *J* = 7.0 Hz, 6H), 2.20 (s, 6H), 1.37 (t, *J* = 7.1 Hz, 9H). ¹³C NMR (100 MHz, CDCl₃)δ: 8.08, 18.72, 54.62, 56.38, 127.35, 128.06, 133.16, 135.06, 161.86.

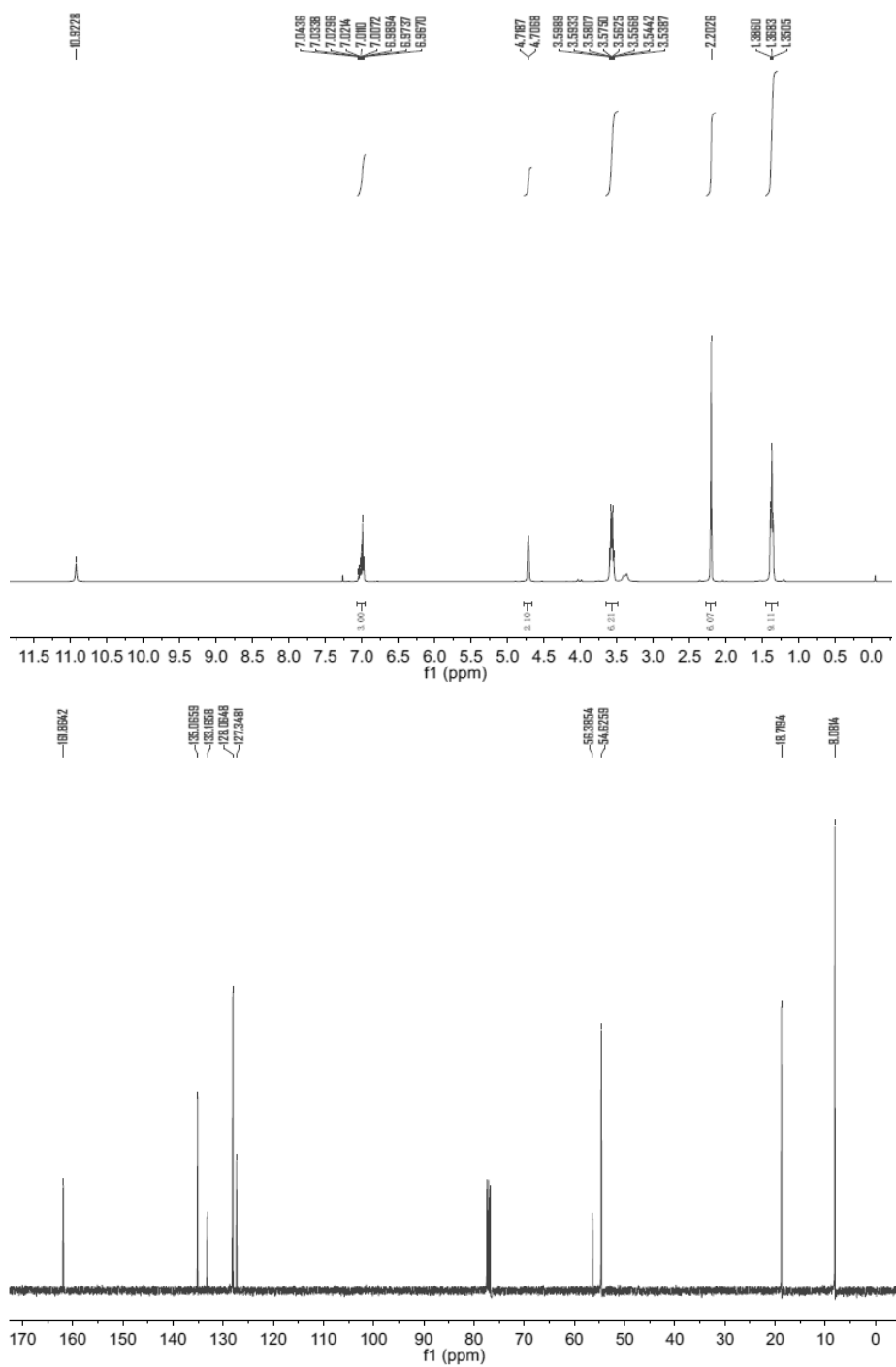
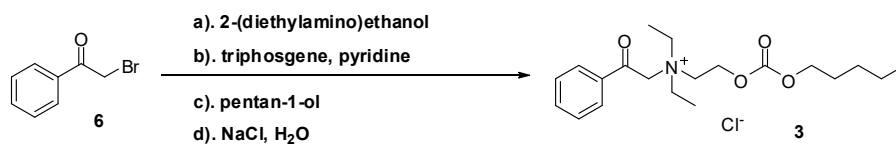


Figure S3 ¹H NMR of compound 2



Synthesis of N,N-diethyl-2-oxo-N-(2-(pentyloxycarbonyloxy)ethyl)-2-phenylethanaminium chloride (3)

Compound **6** (5 g, 25.1 mmol), 2-(diethylamino)ethanol (2.9 g, 25 mmol) and ethanol (20 mL)

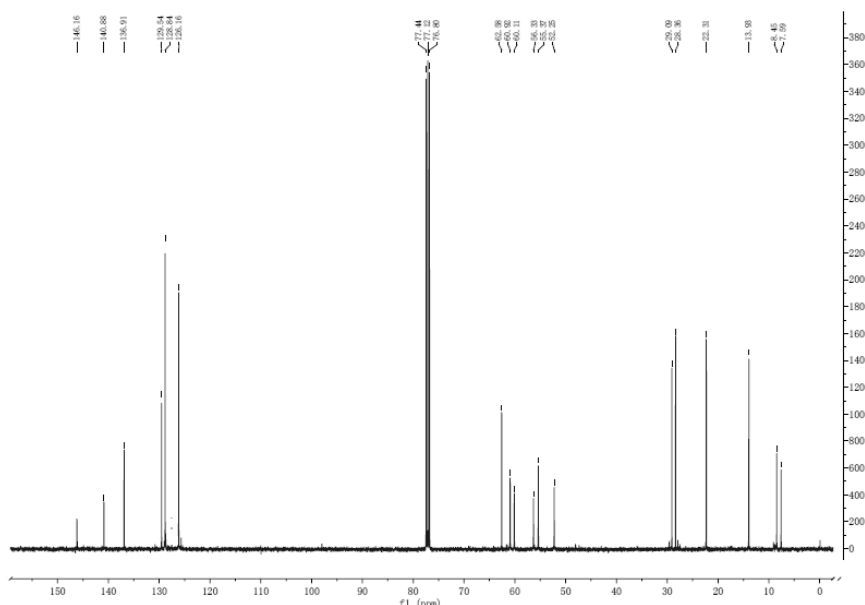


Figure S4 ^1H NMR, ^{13}C NMR of compound **3**

Method on the prapration of (s)-bupivacaine hydrochloride.

HCl in gas form was slightly bubbled into ethanol (500 mL) with ice bath for 30 min. These ethanol solution of HCl was saperately added into (s)-bupivacaine 5.0 g in 10 mL ethanol at $-5\text{ }^\circ\text{C}$ until $\text{pH} < 2.0$. The solvent was evapored. Ehyl actate 30 mL was added, stired and filtered. The residue was washed by ehyl actate 10 mL for 3 times and dried under vano to get white solid.

SI.2 TEM observation

General method on liquid sample preparation

The compound was dissolved in pure water (2 mL) with vigorous magnetic stirring (1000 rpm) at $30\text{ }^\circ\text{C}$ for 12 hours. Some compounds could not dissolve to be a clear solution. All the compound-water mixtures were filtered by needle filter ($0.22\text{ }\mu\text{m}$) to get the solution-like liquid samples.

General method on TEM observation

The liquid sample for TEM observation were prepared by depositing a drop of solution ($100\text{ }\mu\text{L}$) mentioned above onto a 400 mesh copper grid covered with thin amorphous carbon. A drop of phosphotungstic acid (2%, $100\text{ }\mu\text{L}$) was added for negative staining, which lasted for 10 min. Then the sample would be observed by a Hitachi H-600 TEM (120 KV) instrument. Each sample was observed for at least twice.

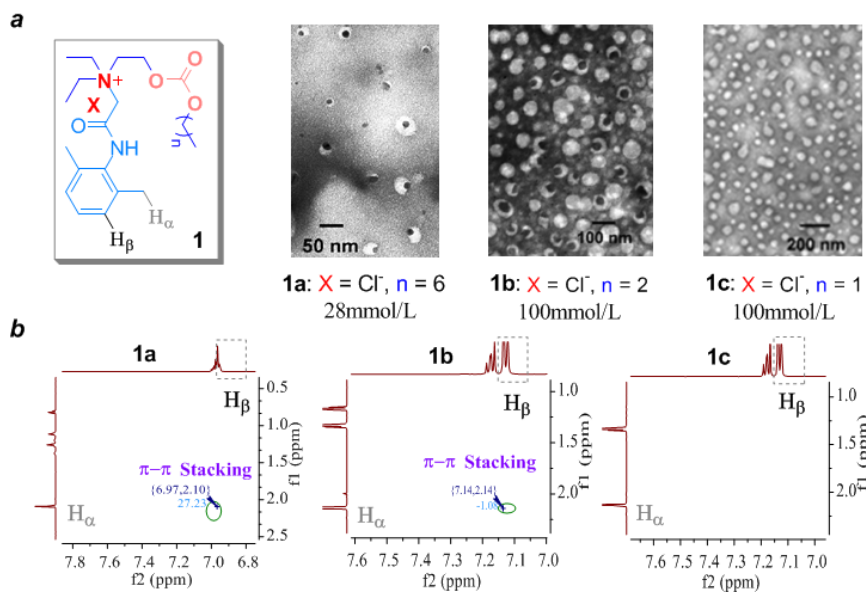


Figure S5 a) Structure and TEM images for **1a**–**1c**. **b)** Intermolecular ¹H–¹H NOESY Spectrum

To ensure whether π - π stacking is directly related to gourd-shaped JPs self-assembled by **1** in water, TEM and intermolecular ¹H–¹H NOESY study similar in our previous work³ were carried out. As shown in Figure S2a and S2b, correlation signal of H_α–H_β representing parallel-displaced π - π stacking¹¹ can be found in JPs systems self-assembled by **1a** or **1b**, but cannot be found in SMs (spherical micelles) system consisted of **1c** with extremely similar structure of **1b** at the same concentration.

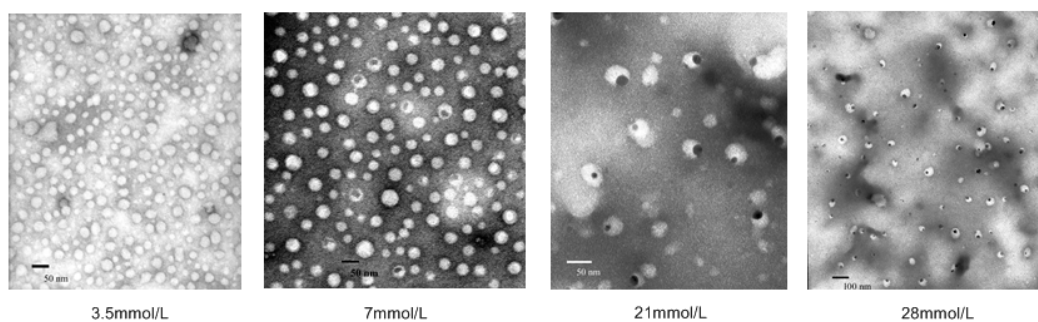


Figure S6 TEM images for **1a** at different concentrations in water

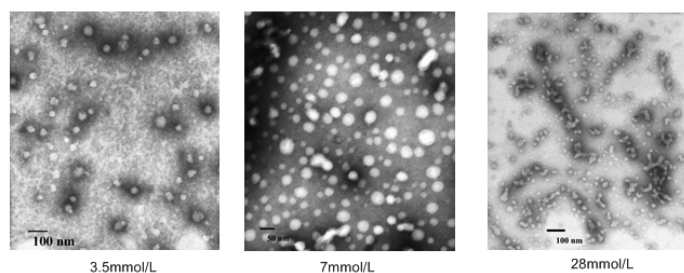


Figure S7 TEM images for **1a** in NS

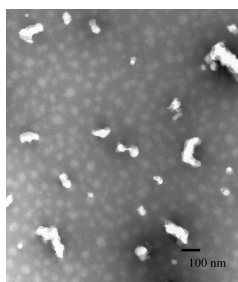
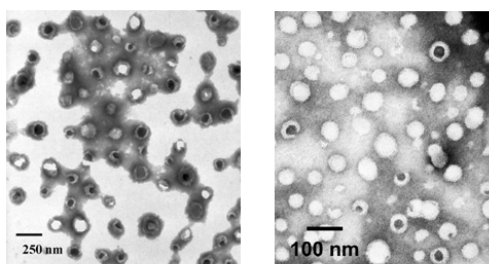


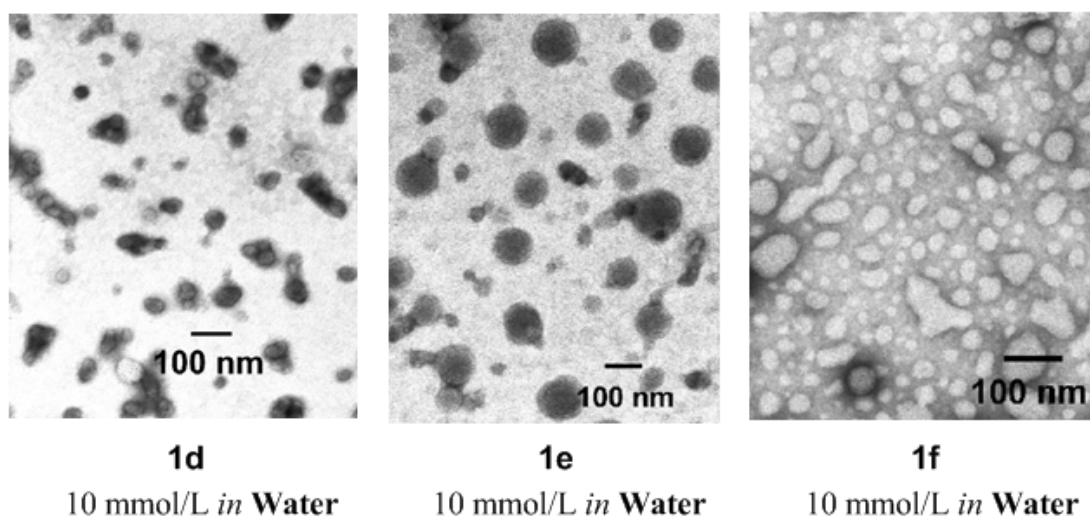
Figure S8 TEM images for **1a** in water at 7 mmol/L with CO₂



2
120mmol/L *in Water*

3
20mmol/L *in Water*

Figure S9 TEM images for **3** and **4** in water



1d
10 mmol/L *in Water*

1e
10 mmol/L *in Water*

1f
10 mmol/L *in Water*

Figure S10 TEM images for **1d~1f** in water

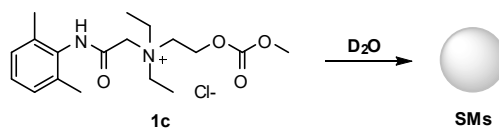
SI.3 2D-NMR analysis

Supramolecular analysis in this part was based on the regulation of gourd-shaped JPs self-assembling of compound **1~3**, which was similar as arrange manner of JPs self-assembled by lidocaine salts. SMs were considered to be arranged in normal way without π - π stacking interaction, and SMs-like particles suggested that they were arranged in similar way of particles formed by **1a** + CO₂ based on PD π - π stacking.

General method for sample preparation

The testing compound was dissolved in D₂O 0.5 mL at approximate concentration as TEM observation. The solution was filtered by needle filter (0.22μm) to get the solution-like liquid samples, and tested by 600MHz NMR.

¹H-¹H NOESY spectrum for 1c:



As shown in Figure S11, we cannot find any correlation between H_α and H_β. Considering to the result that H_α was connected with H_β at same concentration (100 mmol/L) in D₂O and JPs were observed by TEM images in sample of **1b**, we thought π-π stacking was not exist in this nano particle system.

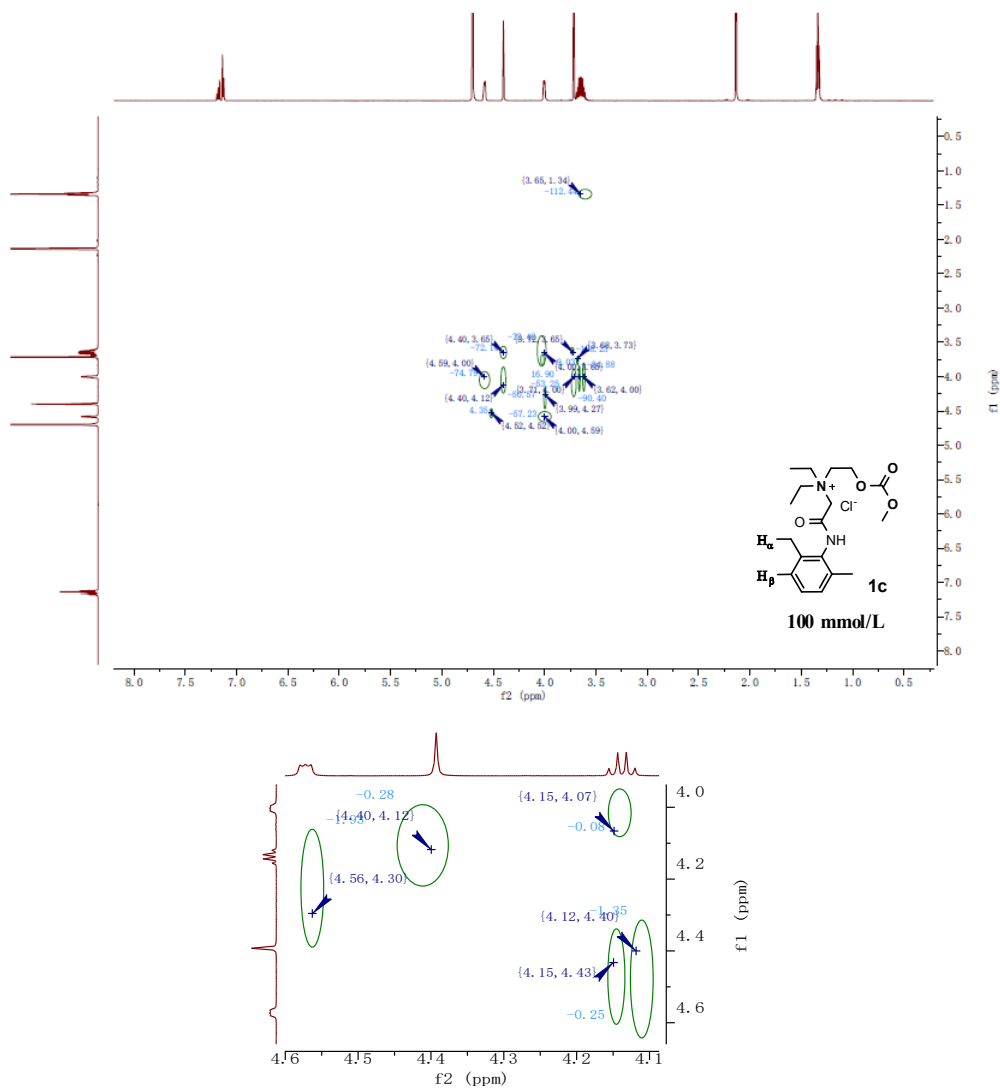
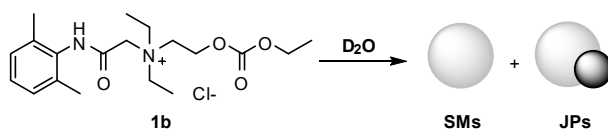


Figure S11 NOESY spectrum for **1c** (100 mmol/L in D₂O)

NOESY spectrum for 1b:



As shown in Figure S12 and Figure S13a, we found H_α was correlated with H_β . Thus, PD π - π stacking was considered to exist. Atypical asymmetric gemini surfactant was indicated by the signal peak of H_c - H_i , shown in Figure S13b.

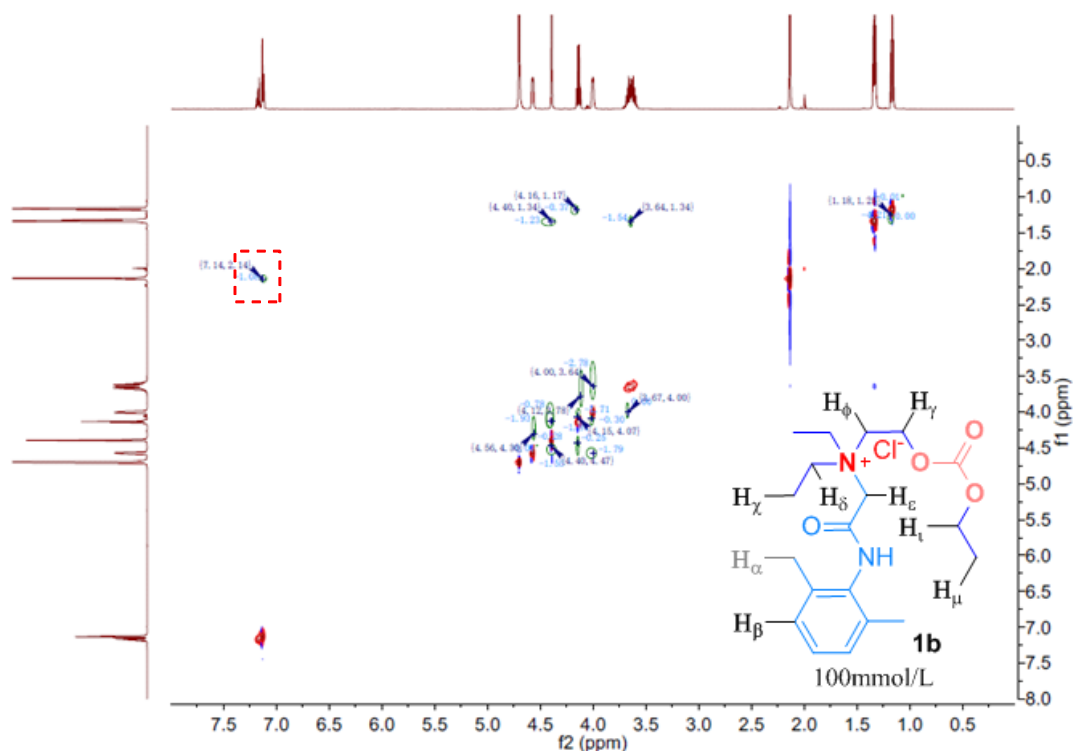


Figure S12 NOESY spectrum for **1b** (100 mmol/L in D₂O)

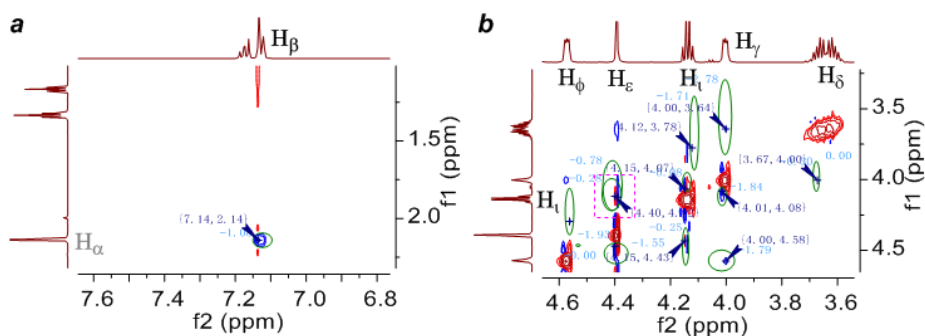


Figure S13 NOESY spectrum for **1b** (100 mmol/L in D₂O)

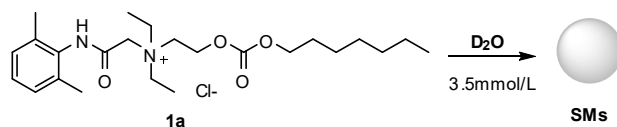
Supramolecular arrangement of JPs self-assembled by **1b** was considered to be in similar

1) Signal peak of H_e was located due to it was the only hydrogen atom correlated to C atom on carbonyl group.

2) Signal peak of H_i was determined because it was the only hydrogen atom related to C atom on alkyl chain, whose chemical shift on ^{13}C NMR was on the range between 20 to 40 ppm.

Determination of these two hydrogen atoms would be of vital importance to the further study of supermolecular structure of nano system self-assembled by **1a**.

NOESY spectrum for **1a**:



In Figure S16, the only two observed signal peaks on cannot provide us more information on supermolecular structure. No correlation between H_α and H_β could be detected on this concentration. This sample would be redetermination after added NaCl 45 mg as the next sample.

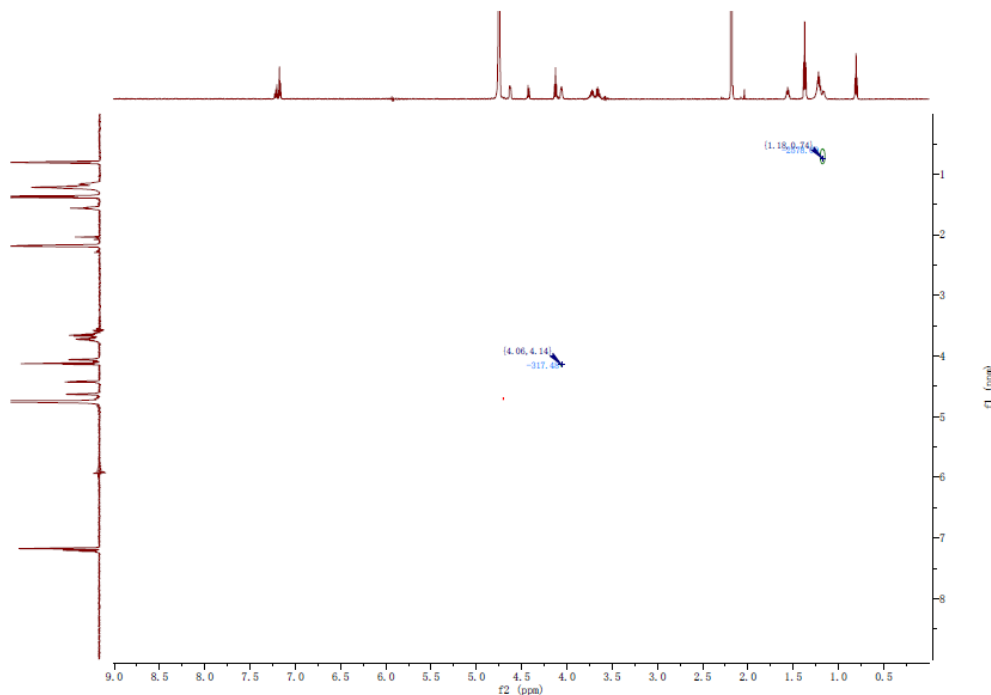
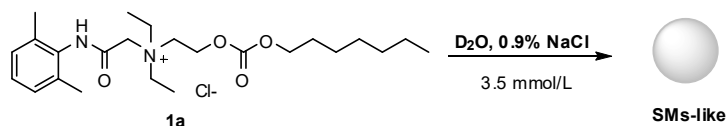


Figure S16 NOESY spectrum for **1a** (3.5 mmol/L in D_2O)



NaCl 45mg was added into the last sample (**1a**, 3.5 mmol/L in D₂O). The tube was shaken several times. This new sample was determined by NOESY in the same condition.

As shown by the NOESY spectrum (Figure S17), the number of signal peaks increased a lot compared to the spectrum in Figure S16. Correlation between H_α and H_β was observed for π-π stacking. Correlations among H_i, H_ε, H_φ and H_γ also indicated that T-shaped π-π stacking was not widely existed in this sample.

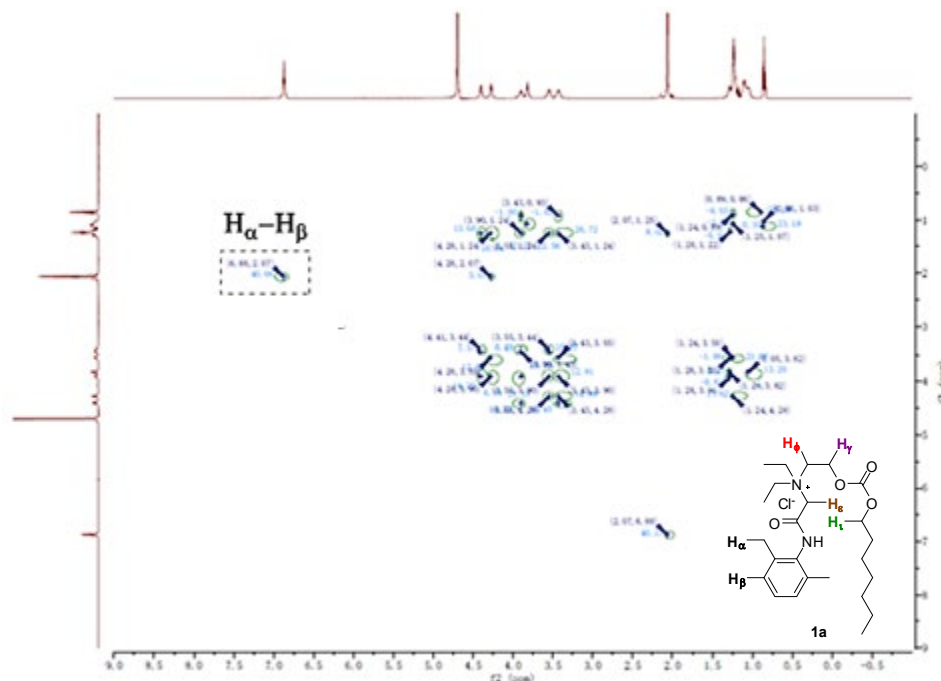
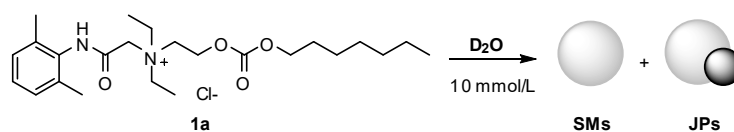


Figure S17 NOESY spectrum for **1a** (3.5 mmol/L in D₂O + 0.9% NaCl)



Although gourd shaped Janus particles were observed in this condition, π-π stacking was not observed in Figure S18. We don't think JPs formation was surely irrelevant with π-π stacking. No signal peak H_α-H_β may also be caused by limited participation of JPs and amount of **1a**. In our opinion, after the concentration increased, this signal peak would be observed.

In this condition, signal peak correlated by H_i and H_ε was clearly observed in Figure S17. In one possible supramolecular arrangement (Figure S19a), the signal peaks lead by relations among H_i, H_ε, H_φ and H_γ cannot be explained. Besides, correlations among H_i, H_ε, H_φ and H_γ also indicated

that T-shaped π - π stacking at least didn't widely exist, otherwise some of these signals would not be detected. However, all the signal peaks in Figure S17 was in accordance with our atypical asymmetric gemini surfactant hypothesis: with the concentration increase, the carbonyl group would move away from hydrophobic region, and the traditional surfactant turned into atypical asymmetric gemini surfactant, and arranged into form **A** caused by parallel-displaced π - π stacking (Figure S19b).

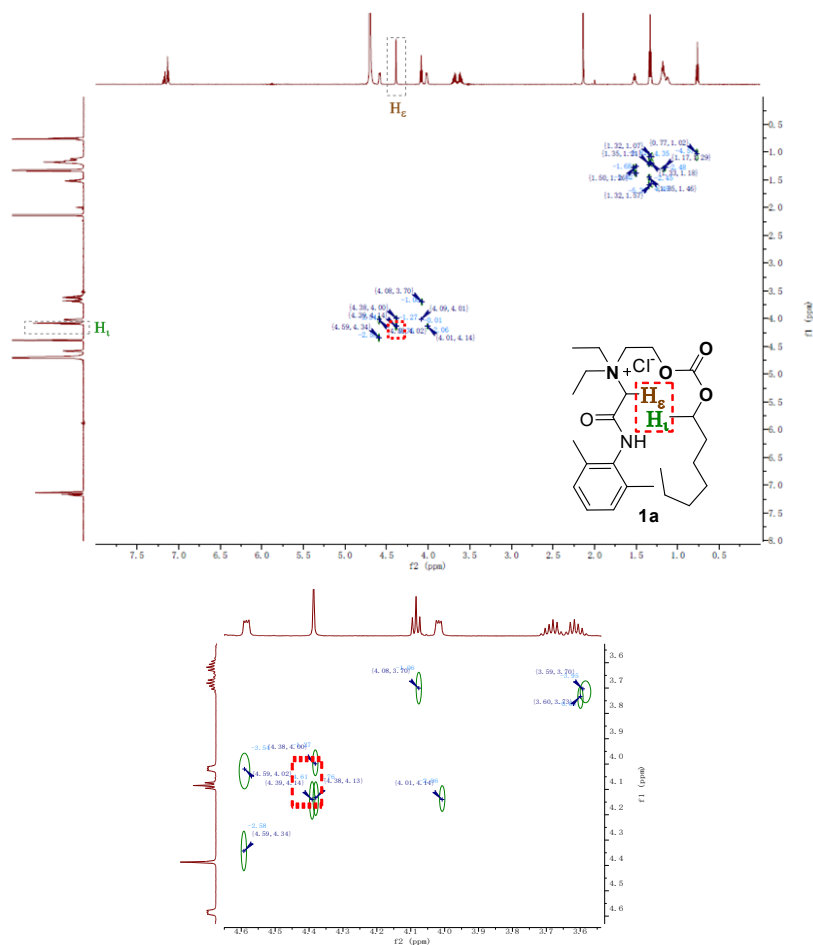


Figure S18 NOESY spectrum for **1a** (10 mmol/L in D₂O)

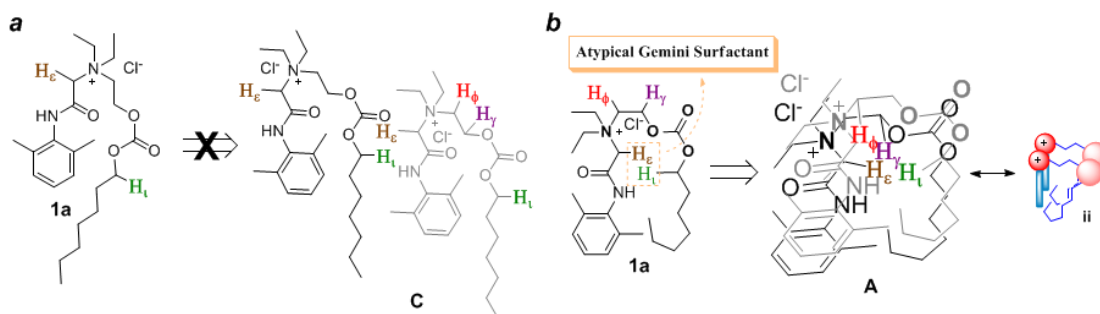
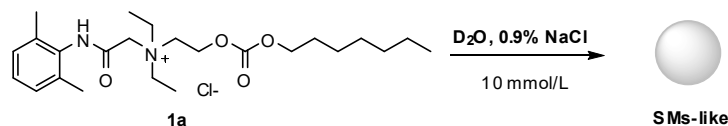


Figure S19 (a) Form **C** was not consistent with NOESY results in Figure S18. (b) Form **A** was in accordance with NOESY results in Figure S18.



NaCl 45 mg was added into the last sample (**1a**, 10 mmol/L in D_2O). The tube was shaken several times. This new sample was determined by NOESY in the same condition.

In Figure S20, the NOESY spectrum was absolutely different from spectrum in Figure S17 (**1a** 10 mmol/L in D_2O). Due to this spectrum was also different from that in Figure S18, SMs observed in this sample were considered to be different in supramolecular arrangement from SMs self-assembled by **1e** at the concentration of 3.5mmol/L in water.

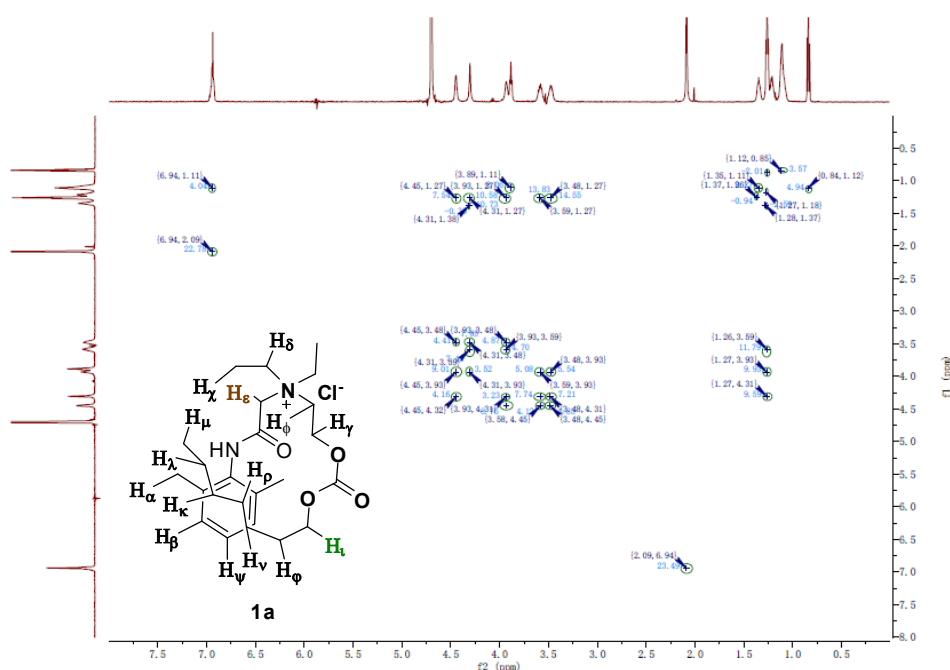


Figure S20 NOESY spectrum for **1a** (10 mmol/L in D_2O + 0.9% NaCl)

As mentioned above, signal peak caused by H_α and H_ϵ was clearly observed in Figure S18 (**1a**, 10 mmol/L in D_2O), which was in accordance with our atypical asymmetric gemini surfactant hypothesis. However, in Figure S20 (**1a**, 10 mmol/L in D_2O + 0.9% NaCl), this signal peak could not be observed (Figure S21c), which indicated that H_α and H_ϵ were no longer close to each other, and carbonyl groups were no longer on the surface of the micelles. Besides, correlation signals among H_ν , H_ϵ , H_ϕ and H_γ also indicated that parallel-displaced π - π stacking would be the dominate manner of π - π stacking, because signals such as H_ϵ - H_ϕ and H_ϵ - H_γ would not be detected in theory when different molecules of **1a** were mainly arranged by T-shaped π - π stacking.

To analyze more informations, we magnified NOESY spectrum in Figure S23, and divided it into 4 parts (Figure 21).

In Figure S21a, two signals could be detected. First, as mentioned above, signal peak (H_α - H_β) indicated π - π stacking. Second, H_ρ , H_κ and H_λ were related to H_β and H_ψ , which implicated that the aliphatic chain was closed enough to H_β and H_ψ on benzene rings.

In Figure S21b, there were 2 groups of key signals. First, H_χ on methyl group was related to all the hydrogen atoms with chemical shift from 3.4ppm to 4.6ppm except H_i , which further illustrated that H_i was no longer close to H_e . Second, H_ρ , H_κ and H_λ were related to H_i , which implicated the manner model iii arranged into model B (Figure S22).

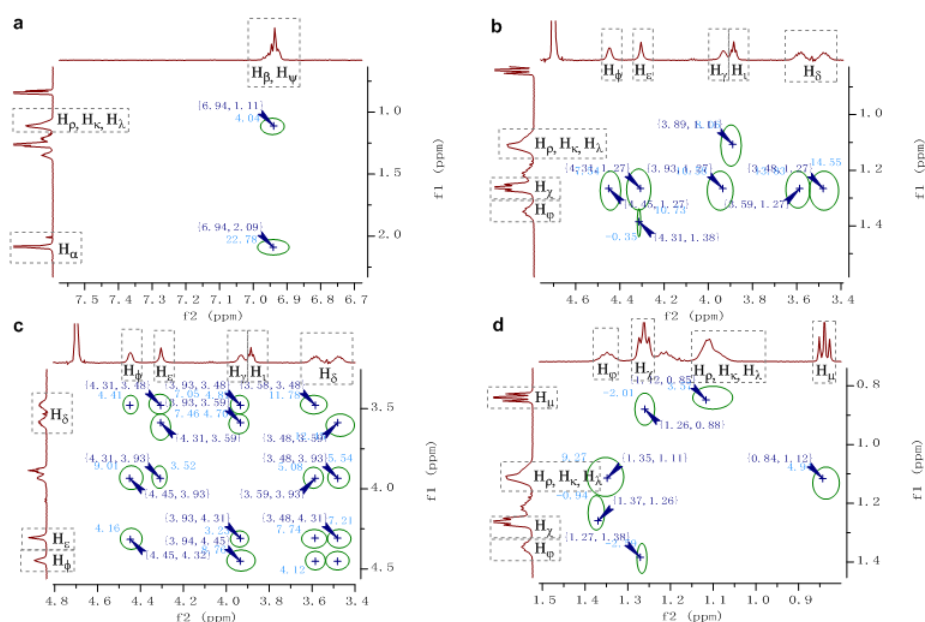


Figure S21 Magnified NOESY spectrum for **1a** (10 mmol/L in D_2O + 0.9% NaCl)

Figure S21d, there were 3 groups of key signals. First, H_χ was related to H_μ , which implicated that methyl group on the aliphatic chain was close enough to methyl group on N-ethyl group. Second, H_χ was related to H_ϕ . Third, H_ϕ were correlated to H_ρ , H_κ and H_λ . The second and third groups of signals indicated how model iii arranged into model **B** (Figure S22).

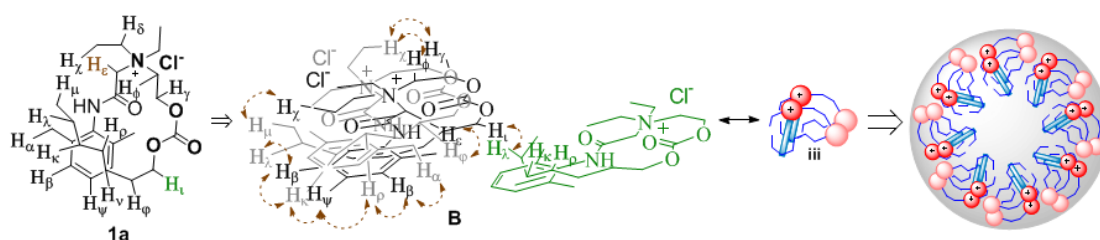
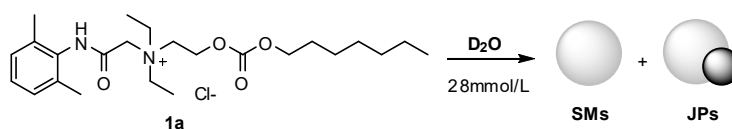


Figure S22 Proposed mechanism on supramolecular structure for **1a** (10 mmol/L in D_2O + 0.9% NaCl)

According to all the analysis on NOESY mentioned above, model **B** was the only possible supramolecular arrangement manner which could match all the NOESY signal peaks for these two samples (**1a**, 3.5 mmol/L in D₂O+0.9% NaCl and **1a**, 10 mmol/L in D₂O+ 0.9% NaCl). Therefore, it was considered by us that SMS-like particles self-assembled by **1a** at concentration of 3.5 mmol/L and 10 mmol/L in NS were consisted by model **B** (Figure S22).



Just as we expected, when the concentration increased from 10 mmol/L to 28 mmol/L, signal peak of H_α-H_β was observed (Figure S23). It indicated the existence of π - π stacking. Different from the NOESY result for **1a** (10 mmol/L in D₂O+ 0.9% NaCl) in Figure S21, no signals caused by hydrogen atom on aliphatic chain and hydrogen atom on aromatic ring was detected, which mean that aliphatic chain was far away from aromatic ring.

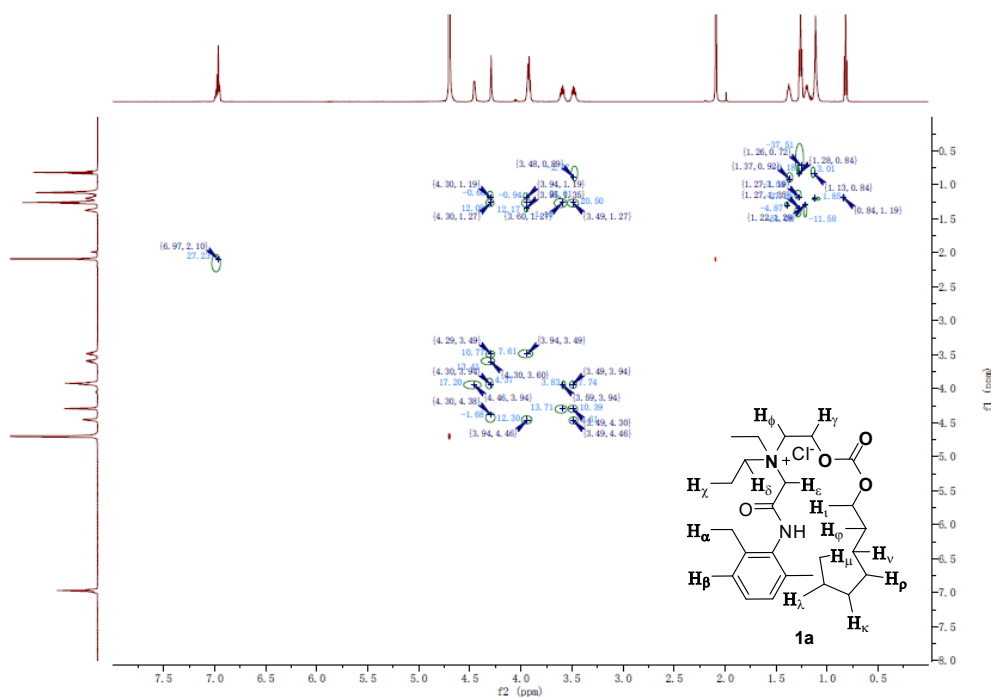


Figure S23 NOESY spectrum for **1a** (28 mmol/L in D₂O)

To analyze the NOESY results for details, we magnified it into 4 parts (Figure S28).

In Figure S24a, as mentioned above, parallel-displaced π - π stacking existed.

In Figure S24b, there were 3 key signals. First, signal of H_ε-H_ν was detected, which was in accordance with our hypothesis: carbonate group was on the surface of the particle. Second, H_μ

was related to H_δ . Third, H_δ were related to H_ρ , H_κ and H_λ . These two results indicated that hydrophobic tail was not only close to the N-ethyl group, but might be curved.

In Figure S24c, there was only one key signal. Due to H_γ and H_i coincided, the relationship among H_e , H_γ and H_i was not clear. Considering to the result above that H_e was related to H_i at the concentration of 10 mmol/L in D_2O in Figure S20, and H_e was related to H_v in Figure S24b, we thought the carbonyl group was still on the surface of this particle. Correlation signals among H_i , H_e , H_ϕ and H_γ also indicated that parallel-displaced π - π stacking would be the dominate manner of π - π stacking.

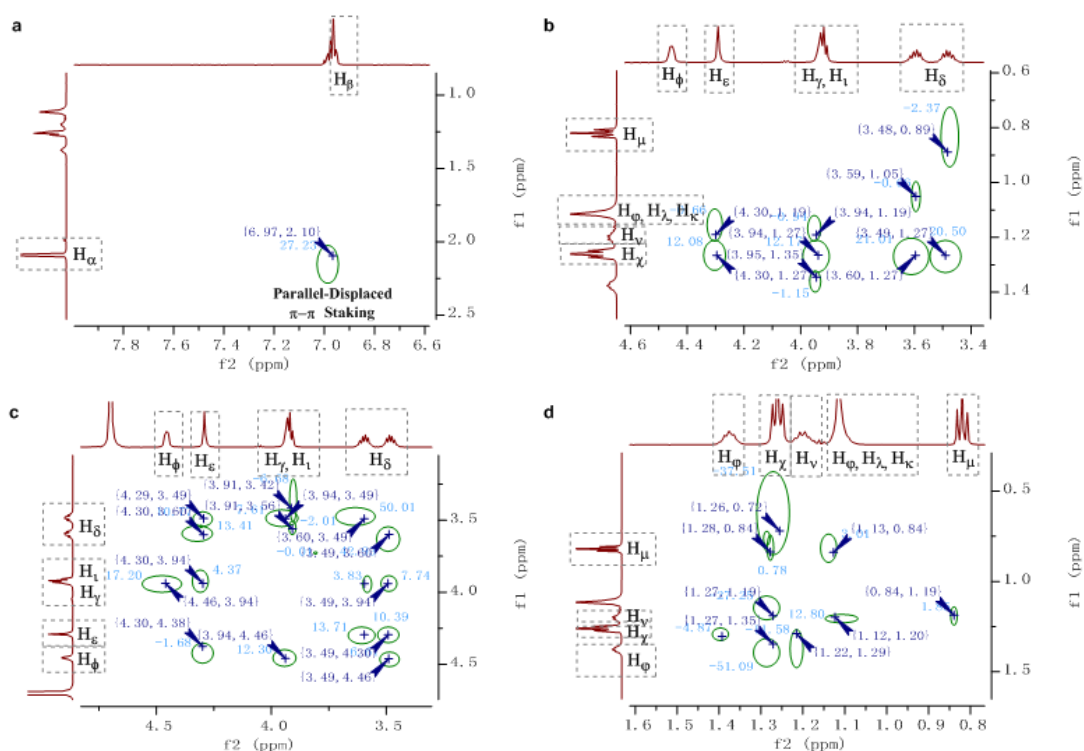


Figure S24 Magnified NOESY spectrum for **1a** (28 mmol/L in D_2O)

In Figure S24d, there were 3 groups of key signals. First, H_μ was related to H_χ . This result confirmed that the bottom of hydrophobic tail was close enough to the N-ethyl group, and the hydrophobic tail was curved. Second, signals of H_μ - H_v and H_χ -(H_ρ , H_κ and H_λ) were observed, which further proved that the hydrophobic tail was curved. Third, signals of H_χ - H_v and H_χ - H_ϕ also proved that hydrophobic tail was close enough to the N-ethyl group.

According to all the analysis on NOESY mentioned above, model **A** was the only possible manner of supramolecular arrangement which could match all the NOESY signal peaks for the result of these two samples (**1a**, 10 mmol/L in D_2O and **1a**, 10 mmol/L in D_2O). Therefore, it was

considered by us that the black sphere of JPs self-assembled by **1a** are consisted by model A (Figure S25). Considering to the result of Figure S16 (NOESY for **1a**, 3.5 mmol/L in D₂O), we thought both the spherical micelles and the white sphere of JPs were consisted by model i as traditional surfactants (Figure S26).

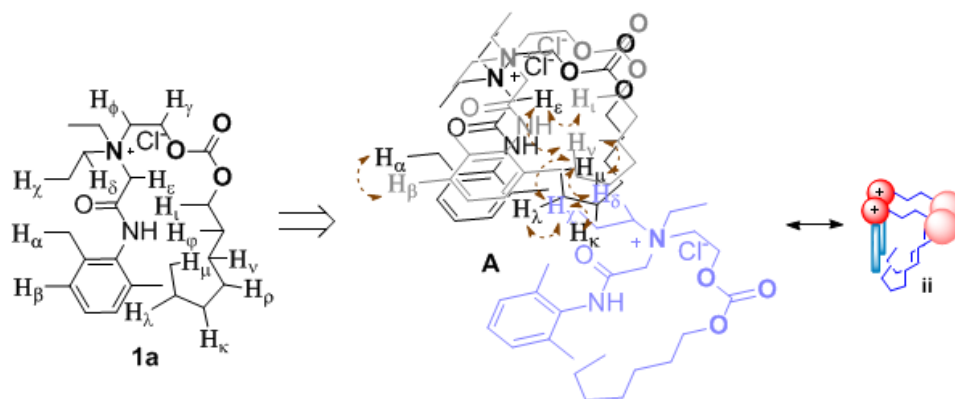


Figure S25 Proposed mechanism on supramolecular structure for **1a** in D₂O

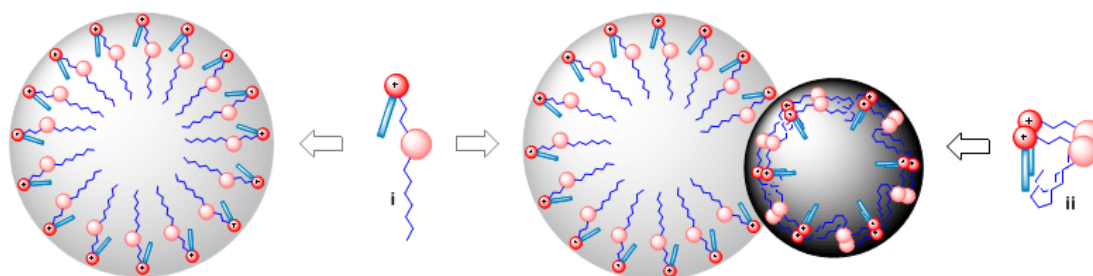
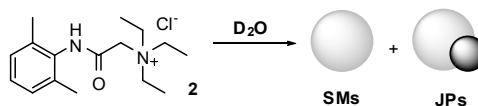


Figure S26 Proposed self-assemble mechanism for **1a** in D₂O (10mmol/L and 28 mmol/L)

Just as we mentioned in previous paper, the color of black sphere was caused by the coordination between tungsten trioxide from the stain and carbonyl group from **1a**. New evidence from NOESY spectrum further proved our previous hypothesis.

NOESY spectrum for 2:



Compound **2** without auxiliary hydrophilic head and hydrophobic tail can also self-assemble into gourd-shaped JPs at 120 mmol/L in water (Figure S9). ¹H-¹H NOESY was carried out at same concentration after water was replaced by D₂O. The spectrum was shown in Figure S27, and magnified in Figure S28.

In Figure S28a, correlation signals of H_α-H_β was observed, which indicated parallel-displaced

π - π stacking.

In Figure S28b, H_ϵ was correlated to H_δ , which was in accordance with parallel-displaced π - π stacking.

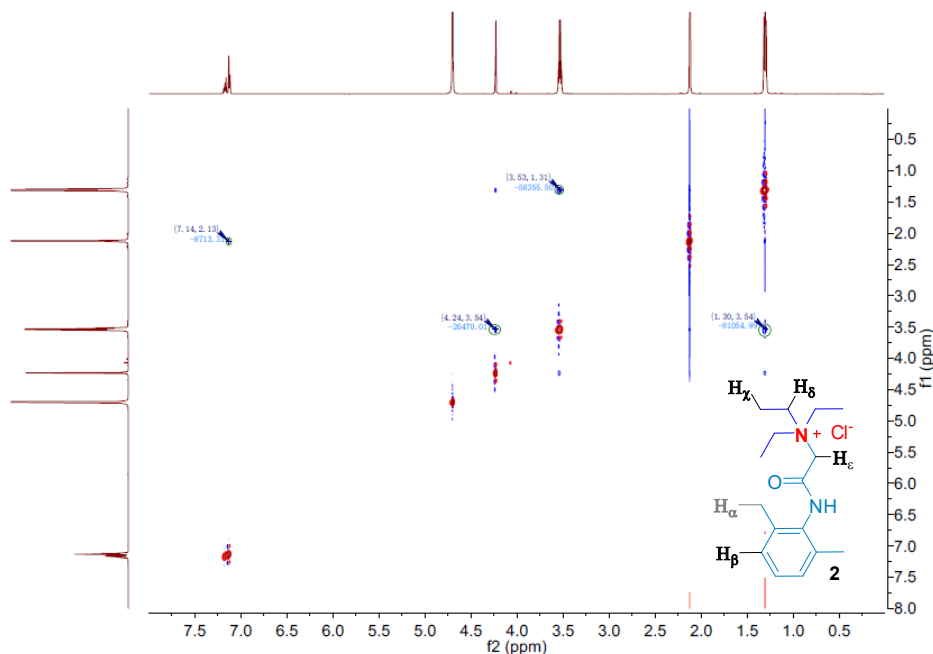


Figure S27 NOESY spectrum for **2** in D₂O

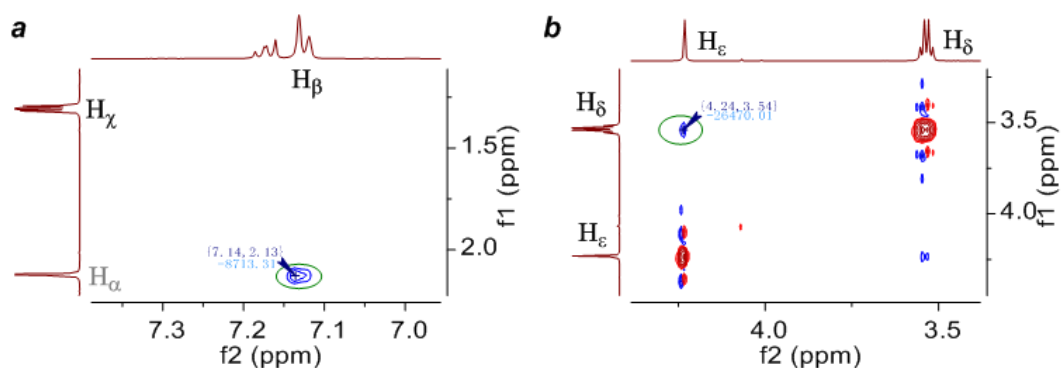


Figure S28 Magnified NOESY spectrum for **2** in D₂O

Based on the data above, model of gourd-shaped JPs similar as those self-assembled by lidocaine hydrochloride or **1a** was established in Figure S29.

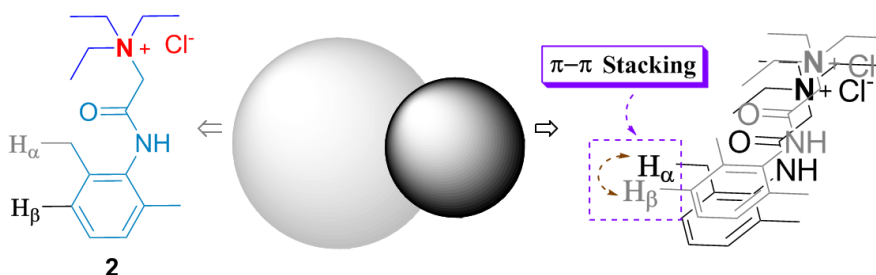
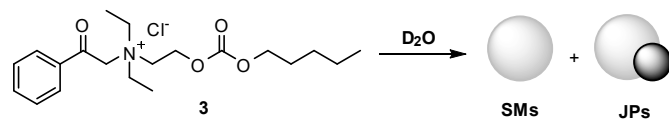


Figure S29 Proposed supramolecular structure of JPs self-assembled by **2**



Due to **3** didn't have methyl group attached to benzene ring, we could not determine the existence of π - π stacking from the signals caused hydrogen atom on methyl group and hydrogen atom on benzene ring. Fortunately, in Figure S30, signal peak H_α -(H_β , H_ω) was observed by NOESY spectrum. Considering only the rig benzene ring on different molecules were close enough in space to each other in a certain manner, H_α on methyl group would be correlated to H_β or H_ω . Thus, this result confirmed that parallel-displaced π - π stacking existed.

Because the signal peaks with the chemical shift from 2.75 ppm to 5.00 ppm in NOESY spectrum for **3** (Figure S30), we cannot make sure whether self-assembling behavior of **3** was in accordance with our atypical gemini surfactant hypothesis. Therefore, we have to locate these hydrogen atom signals by HMBC and ^1H - ^1H COSY analysis first.

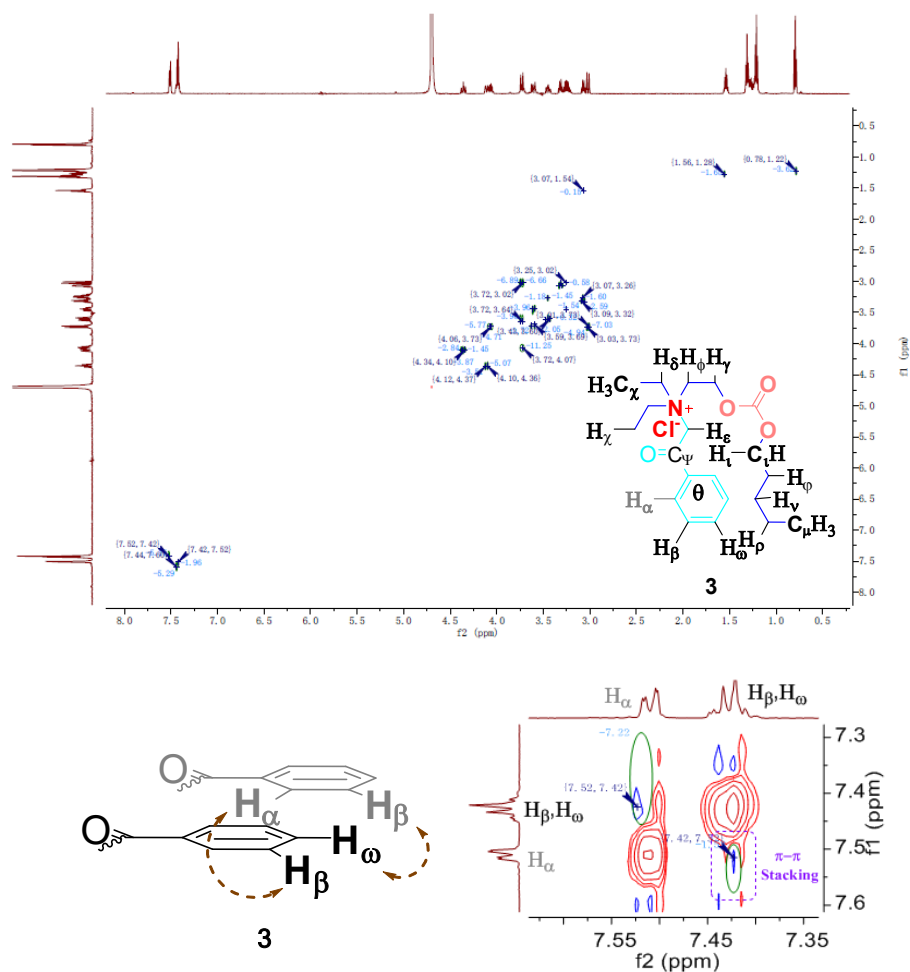


Figure S30 ^1H - ^1H NOESY spectrum for **3**

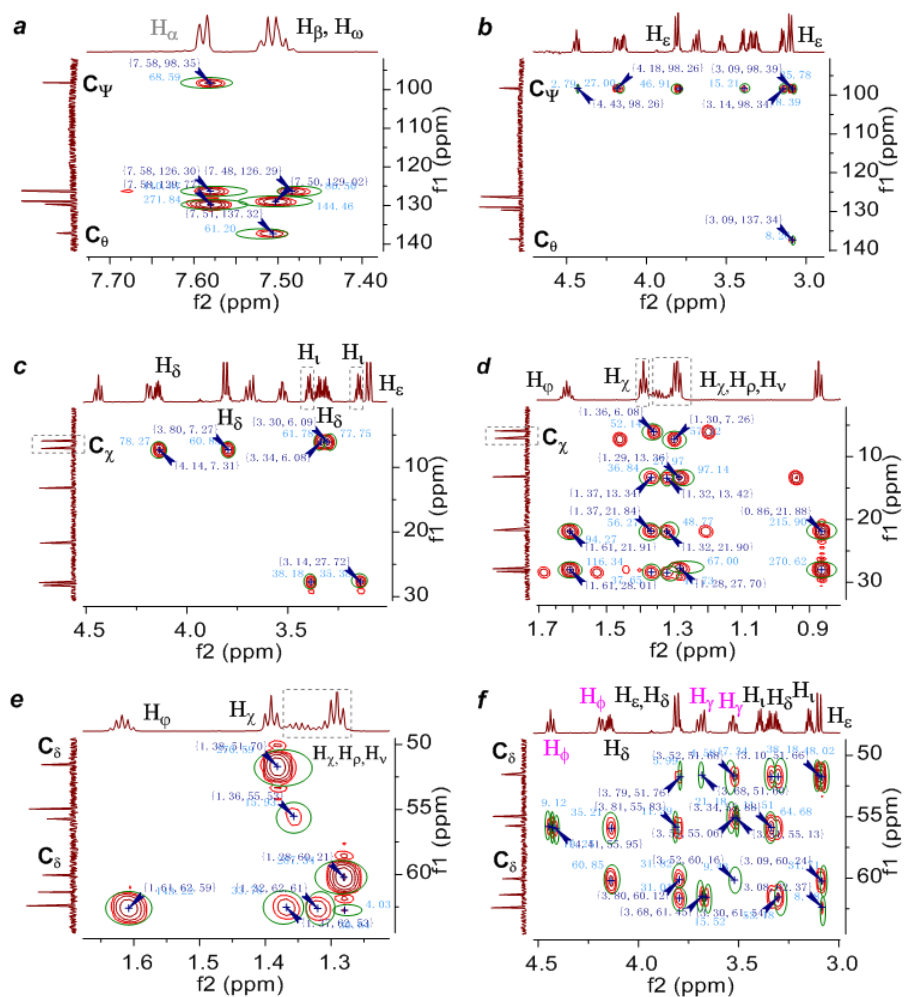


Figure S32 Magnified HMBC spectrum for **3** (16 mmol/L in D₂O)

¹H-¹H COSY spectrum was used for further location (Figure S33).

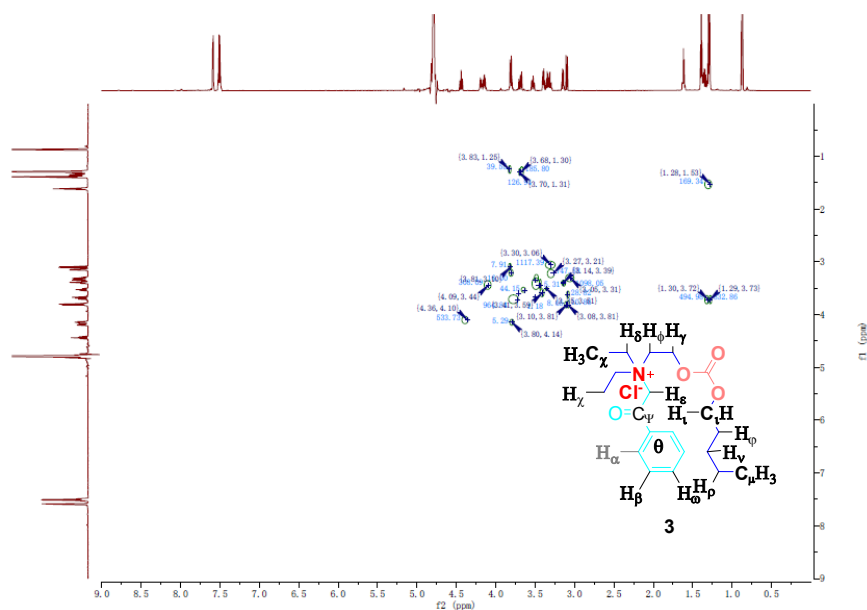


Figure S33 ¹H-¹H COSY spectrum for **3** (16 mmol/L in D₂O)

As shown on Figure S34a, one signal of H_ϕ was re-determined for its correlation to H_χ .

On Figure S34b, all signal peaks of H_ϕ , H_γ , H_δ , H_ϵ and H_i were located by us. Location of H_ϵ and H_i would be of critical importance on the following analysis of NOESY spectrum for **3**.

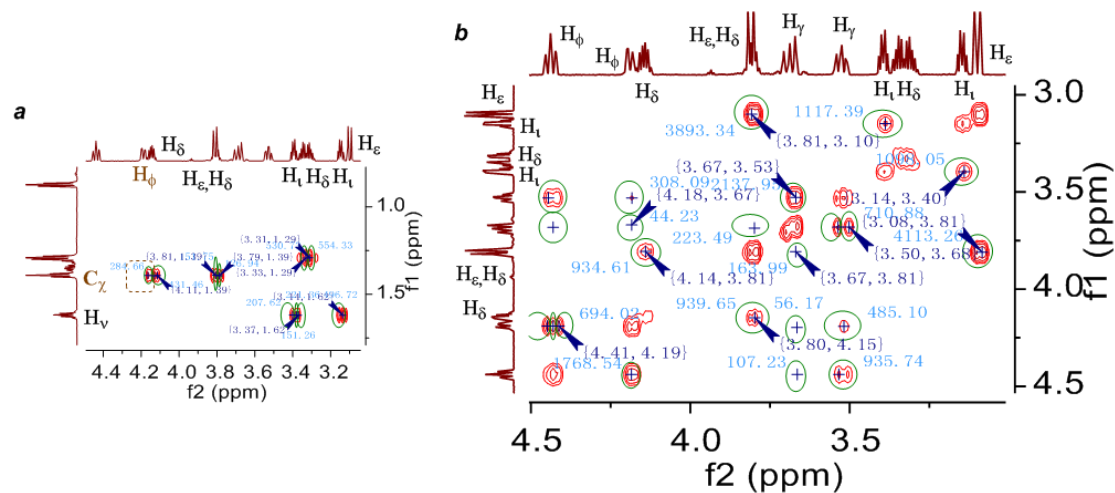


Figure S34 Magnified ^1H - ^1H COSY spectrum for **3** (16 mmol/L in D_2O)

Based on the analysis results of HMBC and ^1H - ^1H COSY above, H_i and H_ϵ were located. From the magnified NOESY spectrum for **3** (Figure S35b), the signal peaks of H_i - H_ϵ was observed, which suggested that self-assembling behavior of **3** in water was in accordance with our atypical gemini surfactant hypothesis.

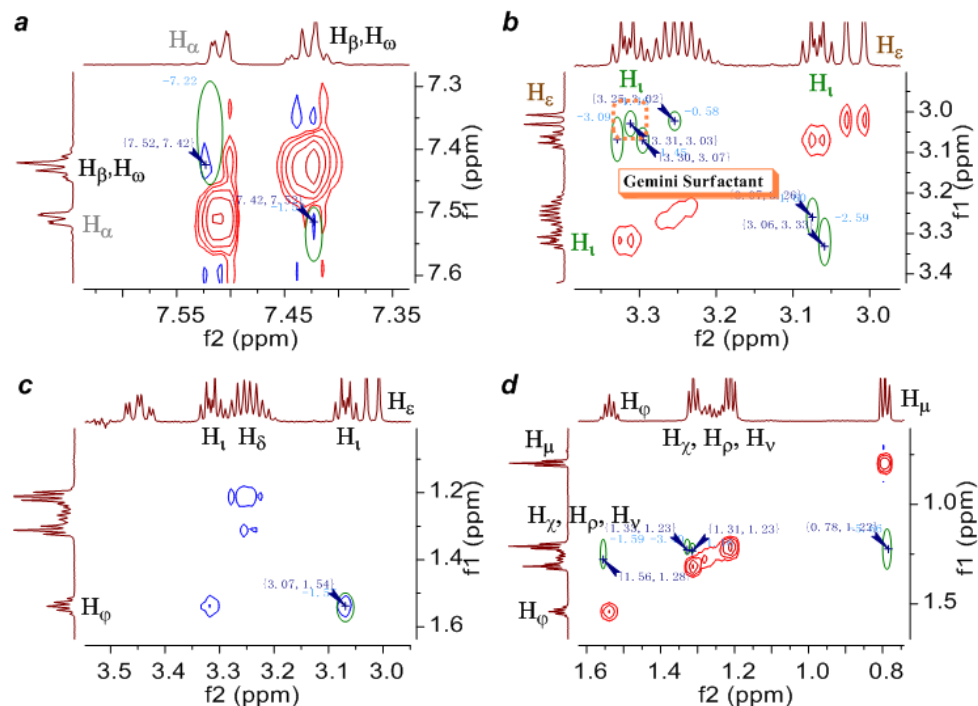


Figure S35 HMBC spectrum for **3** (16 mmol/L in D_2O)

Besides, correlation signals among H_α , H_β and H_χ further suggested that **3** was not arranged by T-shaped π - π stacking, but mainly by parallel-displaced π - π stacking (Figure S36). If different molecules of **3** were arranged by T-shaped π - π stacking, H_β would be far away from H_α and H_ω on another molecule and correlation signals would not be detected.

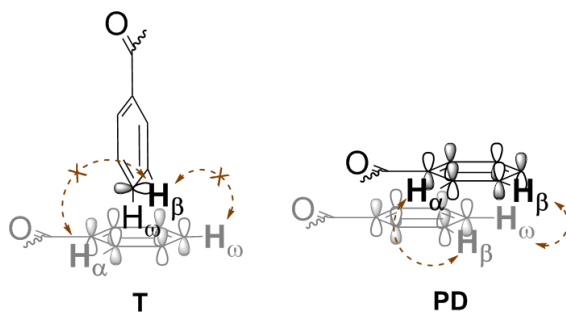


Figure S36 Parallel-displaced π - π stacking for **3** (16 mmol/L in D_2O) was favored.

Supramolecular model self-assembled by **3** in water was proposed in Figure S37, which was similar to model in Figure S29.

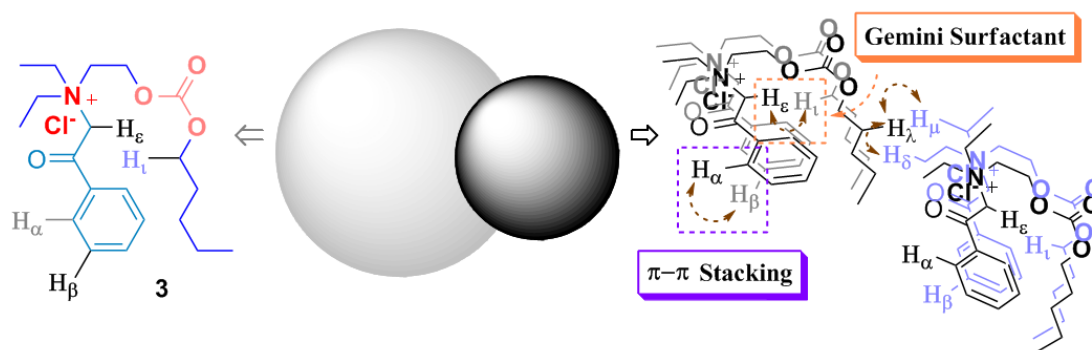
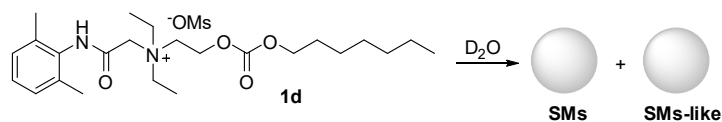


Figure S37 Proposed model of JPs self-assembled by **3**.



As shown in Figure S10 above, **1d** can self-assemble into nano particles with similar shape of SMs. It was suggested by the correlation signal of H_α - H_β in Figure S38 and Figure S39a that π - π stacking existed in this nano system. The area of H_α - H_β was 57.06 approximate to this value for **1a** at 10 mmol/L in water (61.99). In that condition, **1a** self-assembled into SMs and gourd-shaped JPs with π - π stacking interaction. Thus, this nano system was suspected to be consisted of two types of particles: SMs and SMs-like nano particles with π - π stacking interaction.

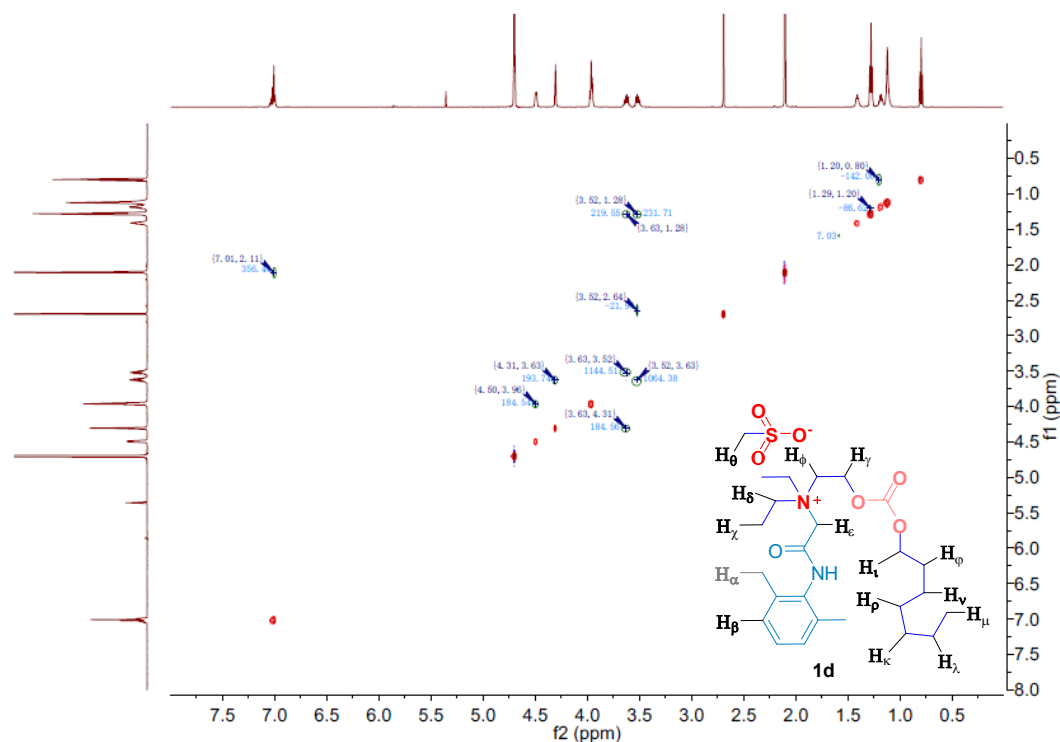


Figure S38 NOESY spectrum for **1d** 10 mmol/L in D₂O.

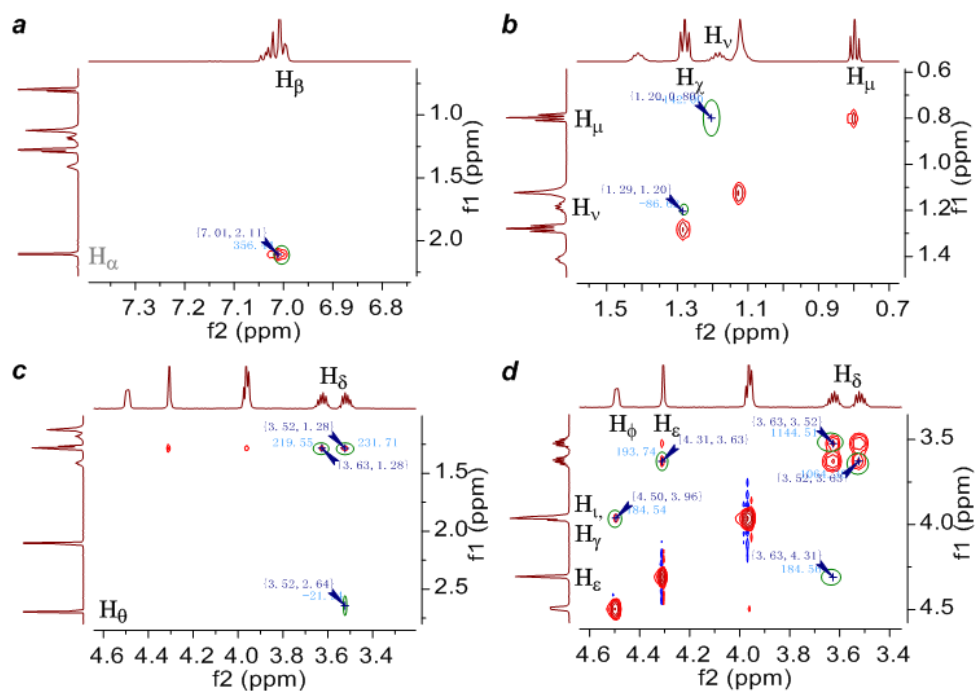


Figure S39 Magnified NOESY spectrum for **1d** 10 mmol/L in D₂O.

In Figure S39b, signal of H_ν-H_μ indicated that these two hydrogen atom were in short distance affected by the curved fatty tail. The connection manner of two different molecules of **1d** was reflected by the signal of H_ν-H_γ.

In Figure S39c, H_δ was observed to be correlated to H_θ , which indicated the relative location of CH_3SO_3^- .

In Figure S39d, no signal of H_ε - H_τ was detected, so that **1d** was irrelevant to the supramolecular structure of atypical gemini surfactant in this nano system. Other signals were in accordance with supramolecular arrangement based on π - π stacking.

Based on the data from NOESY above, supramolecular model of SMs-like particles was proposed in Figure S40, which was similar to the model in Figure S26. SMs in this system were considered to be arranged in normal manner (Figure S41).

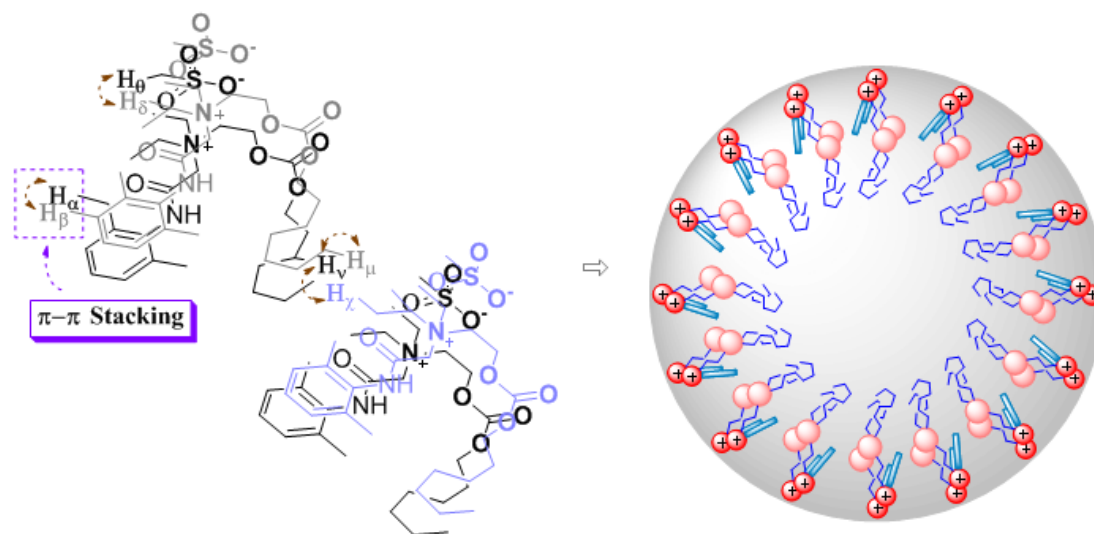


Figure S40 Proposed model of SMs-like particles self-assembled by **1d**.

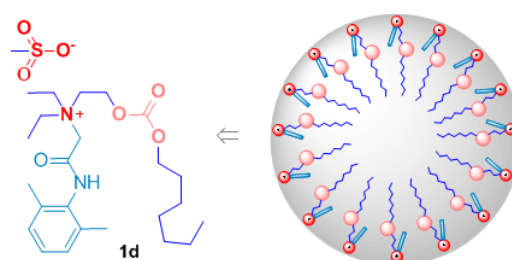
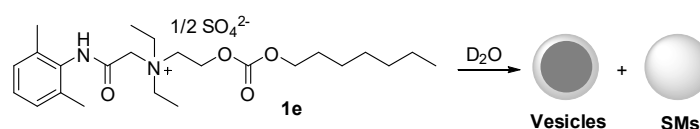


Figure S41 Proposed model of SMs self-assembled by **1d**.



As described in SI.1, counter ions of **1e** were not pure SO_4^{2-} , but a mixture of SO_4^{2-} and HSO_4^- . The actual ratio of SO_4^{2-} : HSO_4^- was 2.8 : 1. NOESY spectrum of this sample was shown in Figure S42.

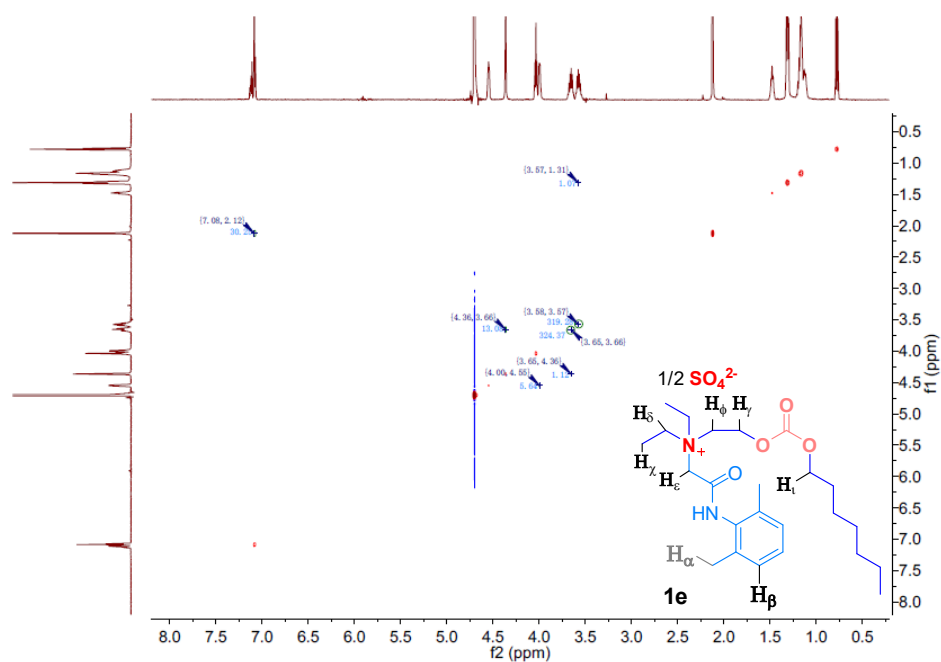


Figure S42 NOESY spectrum for **1e** at 10 mmol/L in D₂O.

Chemical structure of **1e** and its simplified diagram were shown in Figure S43a, and intermolecular ¹H-¹H NOESY spectrum in Figure 42 were partly magnified in Figure S43b~S43d.

In Figure S43b, π - π stacking was proved by the signal of H _{α} - H _{β} . In Figure S43c and Figure S43d, all correlation signals were in accordance with our proposed supramolecular model based on π - π stacking in Figure S42.

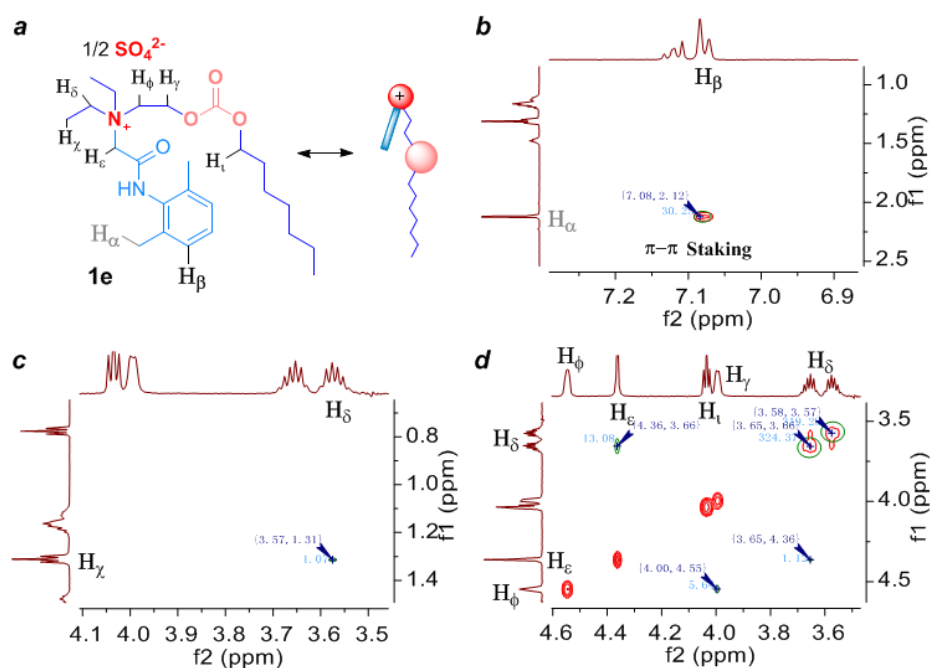


Figure S43 Chemical structure and NOESY spectrum for **1e** at 10 mmol/L in D₂O.

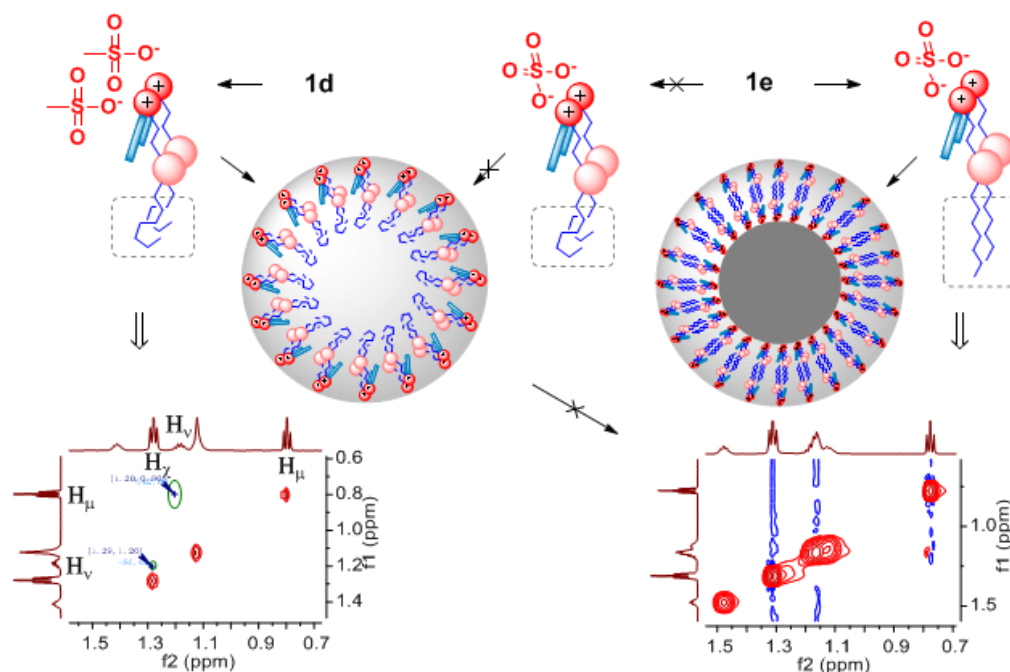


Figure S45 Proposed supramolecular model for **1e** at 10 mmol/L in D₂O.

According to the results above, supramolecular arrangement of **1e** in water was proposed in Figure S46. **1f** with counter ions of HSO₄⁻ was suspected to be arranged in normal way of SMs, and vesicles were considered to be self-assembled by **1e** with counter ions of SO₄²⁻ based on intermolecular π - π stacking interaction. The hydrophobic tail in this nano systems mainly existed in a relax state.

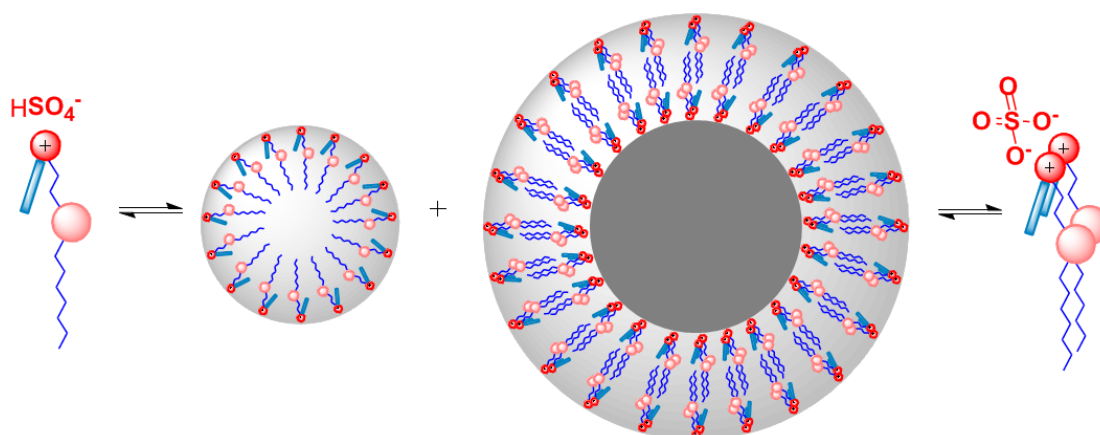
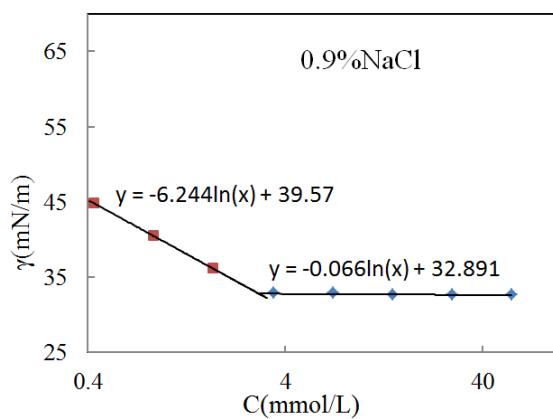


Figure S46 Proposed supramolecular model for **1e** at 10 mmol/L in D₂O.

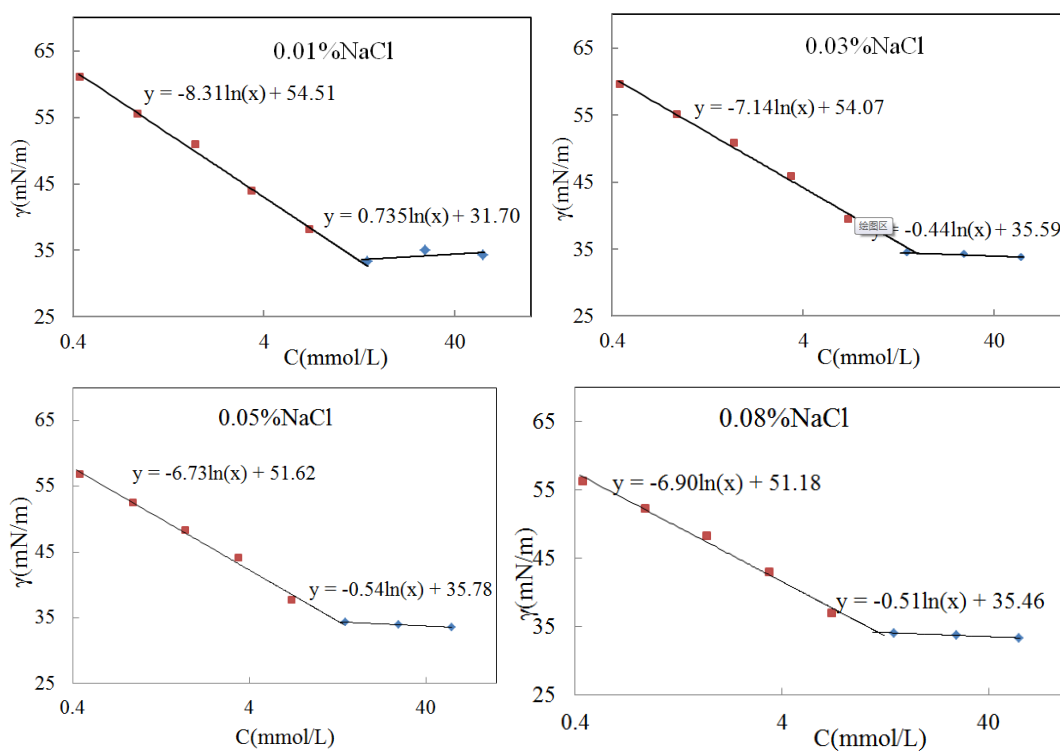
In conclusion, gourd-shaped Janus particles self-assembled by **1**~**3** was proved to be relevant to intermolecular π - π stacking, which was also influenced on the formation of SMs-like nano particles or vesicles.

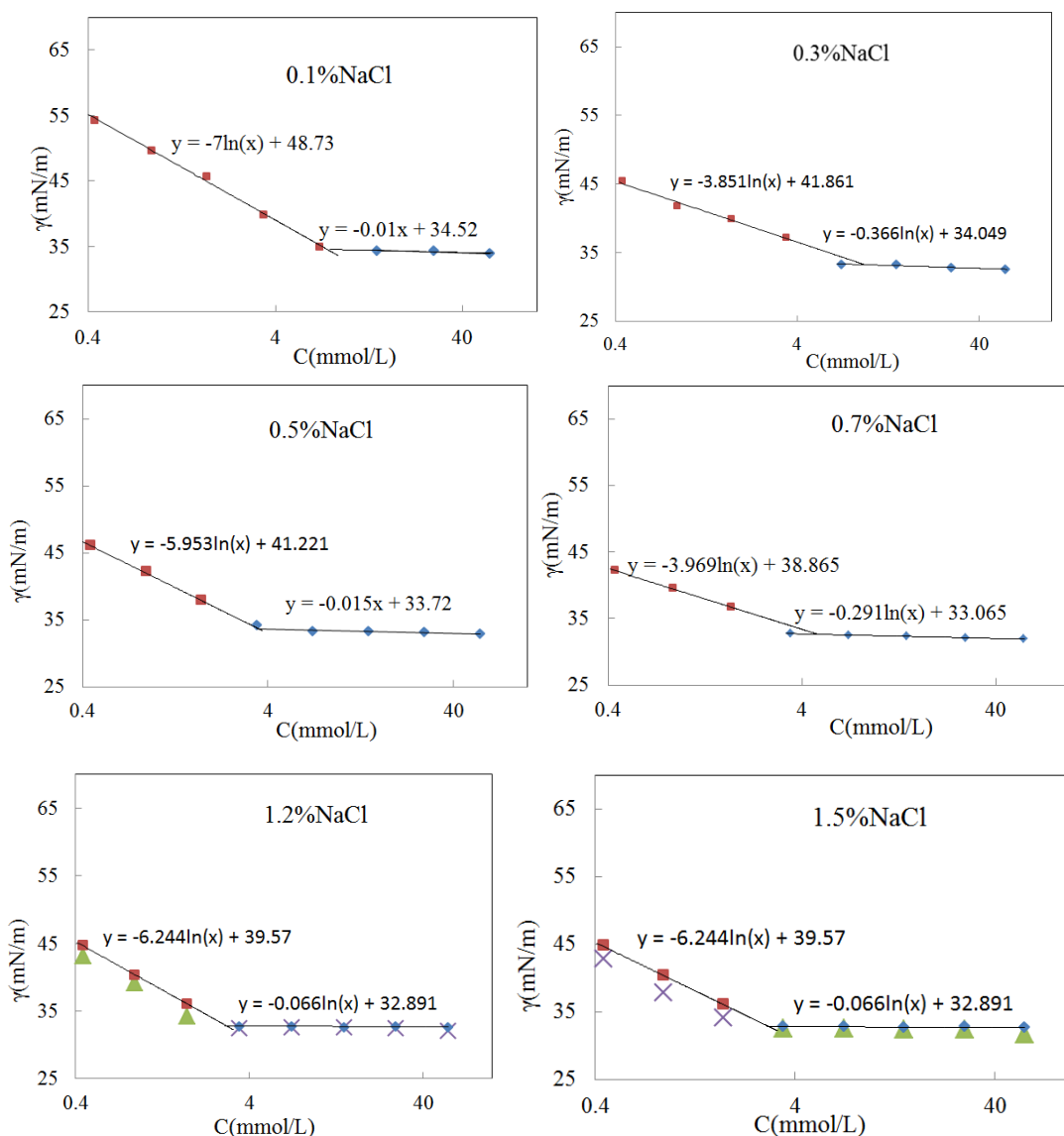
28	32.7	32.7	32.7	32.8	32.8	32.74
14	32.6	32.6	32.6	32.7	32.7	32.64
7	32.9	32.7	32.8	32.8	32.8	32.8
3.5	32.8	32.8	32.8	32.8	32.8	32.8
1.75	36.2	36.2	36	36	36.1	36.1
0.88	40.3	40.5	40.5	40.2	40.1	40.32
0.44	44.7	44.8	44.5	45	44.6	44.72



CMC = 2.83 mmol/L

Scheme S3 CMC of **1a** in NS calculated by surface tension





Scheme S4 CMC determine of **1a** in different concentration of NaCl solution

In conclusion, with the concentration of NaCl increase, the cmc value of **1a** solution decreased significantly. The surface tension of solution at cmc was almost invariant, as shown in Table S3.

Table S3 Surface tension and cmc value of **1a** in NaCl solution

NaCl%	0.01	0.03	0.05	0.08	0.1	0.3	0.5	0.7	0.9	1.2	1.5
CMC (mmol/L)	12.45	15.77	12.92	11.70	7.63	9.40	3.54	4.86	2.83	2.25	2.06
B1 (γ_{CMC}) (mN/m)	33.55	33.63	34.40	34.21	34.50	33.20	33.70	32.60	32.83	32.77	32.75

The CMC values of **1a** in water with different amounts of NaCl additives were presented visually in Figure S47. The CMC value of **1a** in NS (0.9%NaCl in water) was 2.83 mmol/L, which

was much lower than 16.17 mmol/L as the value of **1a** in pure water. The surface tension values of these nano systems at CMC were almost identical, which were in the range of 32.60 to 34.40 mN/m.

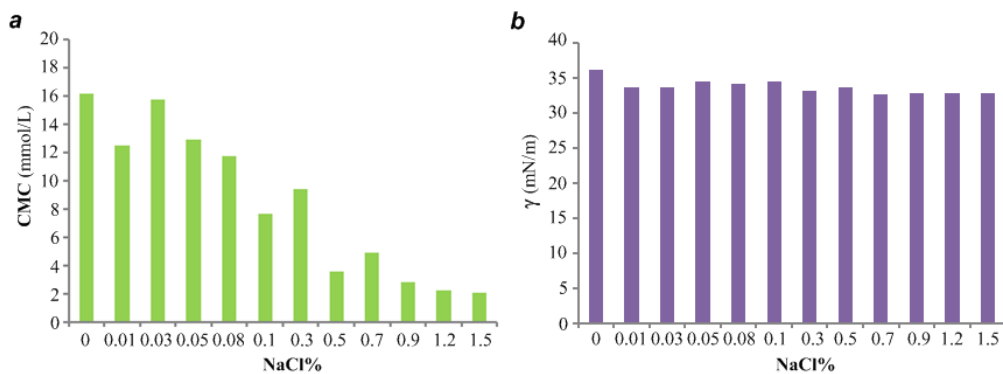
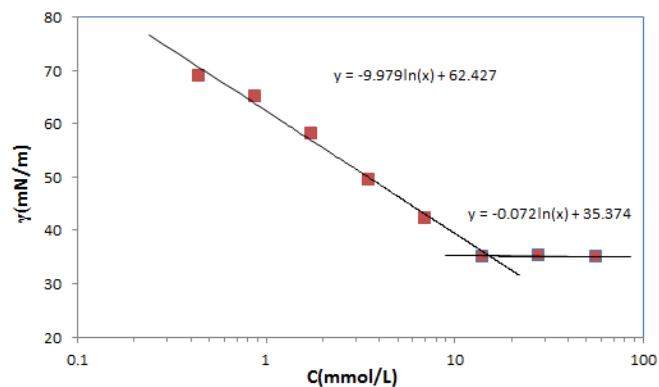


Figure S47 a) Concentration scope of NaCl contains in water on CMC determination of **1a**. b) Concentration scope of NaCl contains in water on surface tension determination of **1a** at CMC.

Table S4 Surface tension determination of **1a** in water bubbled with CO₂

Temperature: 24°C Surface Tension for Pure Water: 73.6 mN/m

Conc. (mmol/L)	Surface Tension (mN/m)					Mean
	Run 1	Run 2	Run 3	Run 4	Run 5	
56	35	35.1	35	35	35	35.02
28	35.2	35.3	35.3	35.3	35.3	35.28
14	35.1	35.1	35.1	35.1	35.1	35.1
7	42.3	42.2	42.3	42.2	42.3	42.26
3.5	49.8	49.7	49.7	49.6	49.5	49.66
1.75	58.3	58.5	58.4	58.3	58.2	58.34
0.88	65.2	65.3	65	65.2	65.1	65.16
0.44	68.8	69	69	68.9	69	68.94



CMC = 15.33 mmol/L

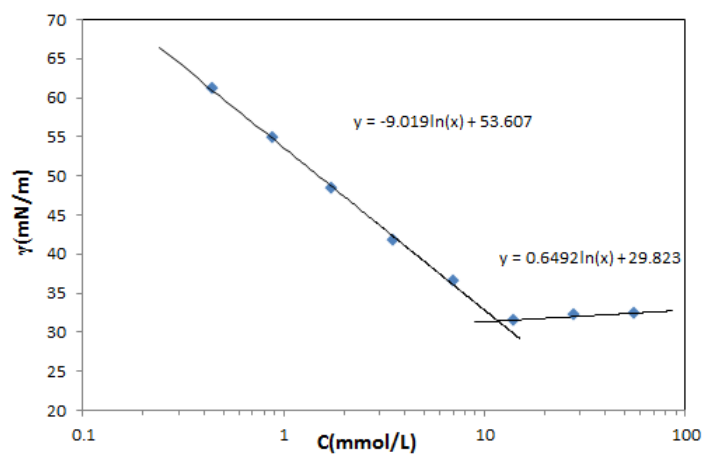
Scheme S5 CMC of **1a** in water bubbled with CO₂ calculated by surface tension

Table S5 Surface tension determination of **1d** in pure water

Temperature: 24°C

Surface Tension for Pure Water: 73.6 mN/m

Conc. (mmol/L)	Surface Tension (mN/m)					Mean
	Run 1	Run 2	Run 3	Run 4	Run 5	
56	32.4	32.5	32.3	32.2	32.3	32.34
28	32.2	32.3	32.1	32.3	32	32.18
14	31.3	31.5	31.5	31.5	31.4	31.44
7	36.5	36.6	36.6	36.6	36.5	36.56
3.5	41.7	41.9	41.8	41.6	41.6	41.72
1.75	48.9	48.1	48.3	48	48.4	48.34
0.88	55.2	55	54.9	54.8	54.9	54.96
0.44	61.6	61.3	61.1	60.7	60.9	61.12



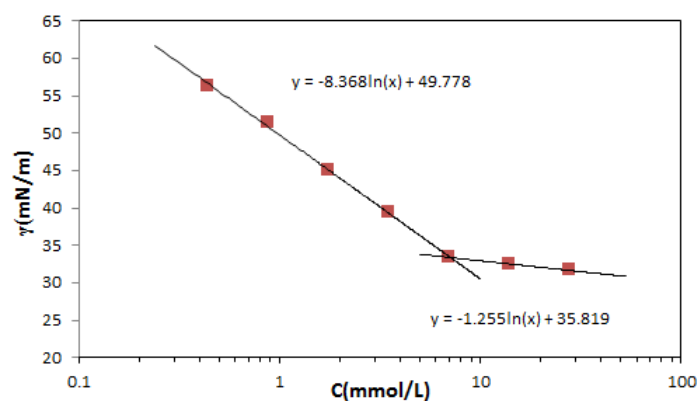
CMC = 11.70 mmol/L

Scheme S6 CMC of **1d** in water calculated by surface tension**Table S6** Surface tension determination of **1e** in pure water

Temperature: 24°C

Surface Tension for Pure Water: 73.6 mN/m

Conc. (mmol/L)	Surface Tension (mN/m)					Mean
	Run 1	Run 2	Run 3	Run 4	Run 5	
28	31.4	31.7	31.6	31.8	31.7	31.64
14	32.4	32.4	32.6	32.5	32.6	32.5
7	33.4	33.5	33.5	33.4	33.1	33.38
3.5	39.3	39.4	39.2	39.3	39.4	39.32
1.75	45.1	45	45	45	45.1	45.04
0.88	51.3	51.5	51.3	51.3	51.3	51.34
0.44	56.2	56.3	56.2	56.4	56.4	56.3



CMC = 7.11 mmol/L

Scheme S7 CMC of **1e** in water calculated by surface tension

In conclusion, CMC value of **1a**, **1d** and **1e** that would be applied in efficacy test were listed in Table S7 separately.

Table S7 CMC value of samples applied for animal test

Sample	1a at 10 mmol/L			1d at 10 mmol/L	1e at 10 mmol/L
	in water	in NS	in water + CO ₂	in water	in water
CMC	16.17 mmol/L	2.83 mmol/L	15.33 mmol/L	11.70 mmol/L	7.11 mmol/L

SI.5 Plasma decomposition measurement

General method on blood trigger test for Figure S48

This operation was aimed to exhibit the safety of **1a**. The experiment condition in this section was selected by us to simulate a clinical procedure in which a local anesthetic was injected to a blood vessel by mistake.

To 5 mL rat plasma in triplicate which were preheated to 37 °C, solution of compound **1a** in water (20 μL, 10 mmol/L) was added and stirred at 1200 rpm/min. The plasma sample (10 μL) was collected at different time points, and added into 40μL acetonitrile-methanol (1:1, v/v) containing 1 μL IS (QX-314, 1 μg/mL). The mixture was vortexed and centrifuged at 2000 rpm for 15 min. The supernatant sample (3 μL) was injected into the LC–MS–MS system. The relevant contents were calculated by the standard curve method, and were then converted into the remaining percentages by dividing the original does.^{S3}

The organic compounds with gemini surfactant structure are always considered to be toxic, and may be in doubt whether they are safe enough for application *in vivo*. To modify the mistakenly

injection into the vessel, nano particle system self-assembled by **1a** in water was added to excessive rat's plasma. It can decompose into compounds with relative lower systemic toxicity in 5 min (Figure S48). With similar gemini-surfactant-like chemical structure, local anesthetics designed for fast-decompose to decrease toxicity were more difficult to decompose in plasma, which needed at least more than 2h to decompose completely (Figure S49).^{S4} The capability of self-assembling was also declined a lot due to the significant decrease of hydrophobic tail.

LD₅₀ (the dose at which 50% of animals die) were measured by intravenous injection on rats' femoral vein according to up and down method^{S3} for six crossovers. The dosage began from 16mmol, and rised 1.25 times for the next test point.^{S5} As control group, (s)-bupivacaine hydrochloride was determined as 5.6 mg/kg on LD₅₀ measurement.

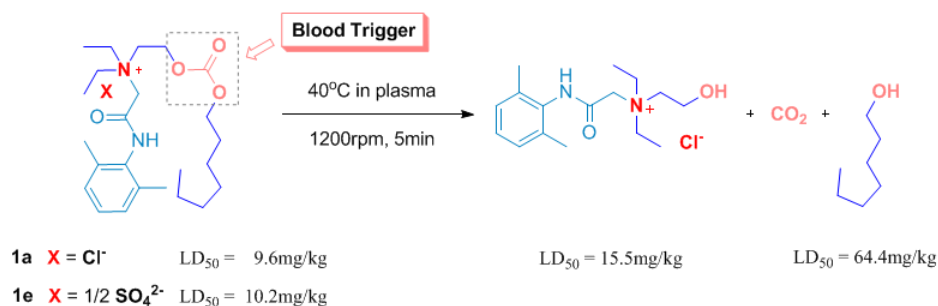


Figure S48 Blood trigger test and LD₅₀ determination of **1a** and **1e**

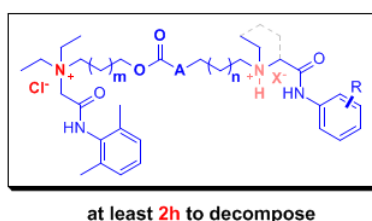


Figure S49 Slow-decompose series-type gemini surfactant with same carbonate group as blood trigger

General method on *in vitro* decomposition test

Exam in this section was aimed to test the stability of **1a** in local tissue after unexcepted contact with small amount of blood during the rats' surgery operation.

To 2 mL rat plasma in triplicate which were preheated to 37 °C, solution of compound **1a** in water (200 μL, 10 mmol/L) was added, vortexed for 1min, and kept without stirring. The plasma sample (100 μL) was collected after the mixture was vortexed for 30 s at different time points, and added into 400 μL acetonitrile-methanol (1:1, v/v) containing 10 μL IS (QX-314, 1 μg/mL). The

mixture was vortexed and centrifuged at 2000 rpm for 15 min. The supernatant sample (3 μ L) was injected into the LC–MS–MS system. The relevant contents were calculated by the standard curve method, and were then converted into the remaining percentages by dividing the original does.^{S6}

LC-MS-MS condition

The LC–MS–MS system consisted of an Agilent 1260 liquid chromatograph and a 6460 triple quadrupole mass spectrometer with an electrospray ionization source. Data were analyzed by MassHunter software (Agilent Corporation, MA, USA). Separation was on an Ultimate XB-C4 column (3.0 mm \times 100 mm i.d., 3 μ m, 300 \AA , Welch Materials, Inc., Maryland, USA) by isocratic elution with 0.1% formic acid/acetonitrile (45:55, v/v), at a flow rate of 0.3 mL/min, and the total run time was 10 min for each injection.

Mass spectrometry conditions were set as follows: sheath gas flow 11.0 L/min; sheath gas heater temperature 300 $^{\circ}$ C, nebulizer pressure 45 psi, capillary voltage 3500 V. Quantification was performed by multiple reactions monitoring (MRM) mode of the transitions at m/z 421 \rightarrow 89.1 for compound **1a**.

Results

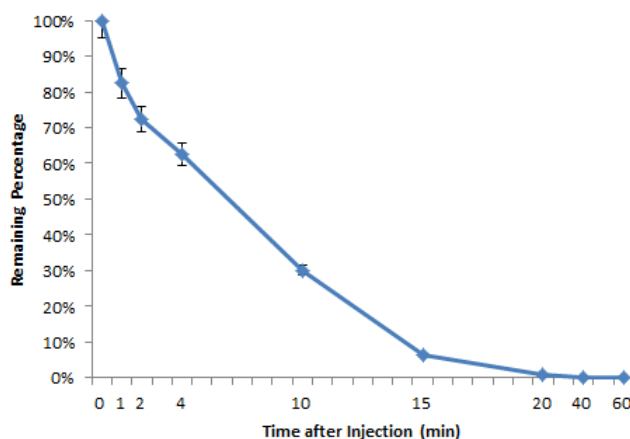


Figure S50 Plasma decompose of **1a** (10 mmol/L in water)

In Figure S50, **1a** was unstable in plasma, especially at relative higher concentration. To keep further test data accurately, we have to try our best to keep our sample away from blood in room temperature, such as washing tissues with water and quick surgery operation at 0 $^{\circ}$ C.

SI.6 Rats' sensory block and neuropathological injury measurement

Rats' sensory block

Sprague Dowley rats (male, Dossy Experimental Animal Company, Chengdu, China) weighted

180~200 g were housed at room temperature and moiety of 40%~60%, in 12h light/12h dark cycle with free access to food and water. Animals were acclimated to experimental environments before tests. During acclimation, baseline of sensory was measured every day for three consecutive days, averaged, and recorded. Those with normal baselines were used, and randomized into groups (n = 8 for each group).

Rats received sciatic nerve block under sedation with inhaled 1.5%~2.0% isoflurane (v/v %) mixing with oxygen. 0.2 ml of test solution was injected through a 27-Gauge syringe that was inserted at the mid-point between trochanter and ischial tuberosity.^{S7} 100% successful rate was obtained with this method using common local anesthetics, and no signs of nerve injury was observed when saline was used in preliminary tests.

Sensation of the injected limb was evaluated after sciatic nerve block by revised hot plate test at 10min, every 2 hours from 2 to 10 hours, and every 8 hours until the sensory block offset for the concentration scope of **1a** in water. For the further study on **1a** in water **1a** in water with CO₂, **1a** in NS and **1d** in water, hot plate test was began at 10min after injection, and hourly from 2 to 5 hours, hourly from 9 hours until the sensory block offset. For the study on **1e** in water, hot plate test began at 10min after inject, and hourly from 36 hours until offset.

The paw withdrawal latency (PWL) induced by heat stimulation represents the degree of sensation block. The baseline of PWL lasted no longer than 3s, and the cutoff time of PWL was set at 12 s to avoid tissue injury. PWL > 6 s was considered effective nociceptive blockade. The time for PWL to exceed 6 s was the onset time of sensory block; the time for PWL to return below 6 s was the offset of sensory block: the interval between onset and offset time was the duration of sensory blockade. Systemic adverse effect was observed during the injection and observation period, and every day within 7 days after injection.



Rats before Injection



Rats 10min after Injection

Figure S51 Typical image of tested rats before and after injection

Results

Concentration scope for **1a** in water was carried out in Figure S52. Considering to the results of sensory block duration, neuropathological injury as well as species of nano particles confirmed by 2D NMR above (SMs and JPs, 4 h duration with no nerve injury at 7 mmol/L; SMs, 18h duration with moderate nerve injury at 14 mmol/L), we chose 10 mmol/L as the concentration of **1a** for further study.

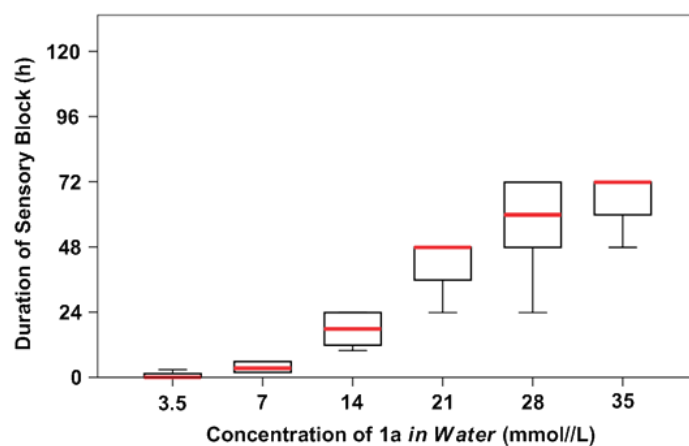


Figure S52 Concentration scope for **1a** in water on rats' sciatic nerve block.

Nerve function of tested rats would be completely recovered after efficacy if these rats were injected by sample of (s)-bupivacaine (0.75%), **1a** in water, **1a** in water with CO₂, **1d** and **1e** in water, as shown in Figure S53a. 50% of tested rats cannot recover after injected by **1a** in NS, which was reflected by curl toes, abnormal gait, and muscle paralysis (Figure S53b). Similar situation occurred after injected by **1f** at 10mmol/L in water. 25% of tested rats cannot recover into normal state.

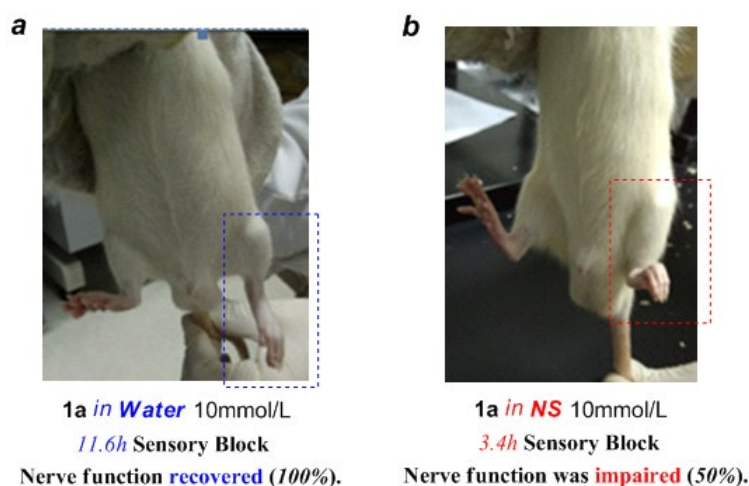


Figure S53 Typical image of tested rats after injection

As shown in Table S8, the duration of sensory block for **1a** self-assemble in pure water was of significant difference from the duration of **1a** in NS. Due to the duration data might be slightly different determined by different operators, all the operation were completed by the same researcher. The rats' behaviors were also observed after sensory block offset as mentioned in manuscript. Nerve function of 4 rats injected by **1a** in NS was impaired, as reflected by curl toes, abnormal gait, and muscle paralysis, while rats injected by **1a** in pure water recovered normally.

3 rats cannot resume into normal after 8 rats were injected by the sample of **1f** were injected, which reflected more serious than performance of rat in Figure S53b. This result was considered to be caused by H⁺ released by HSO₄⁻ with pKa = 3.0. Therefore, sensory block duration cannot be measured accurately, so that this data were not exhibited in Table S8.

Table S8 Sensory block duration

Sample	Sensory Block Duration (hours)								
	Run 1	Run 2	Run 3	Run 4	Run 5	Run 6	Run 7	Run 8	Mean
1a in Water + CO ₂	12	12	13	12	13	12	11	12	12.2
1a in Water	12	11	12	12	12	12	11	11	11.6
1a in NS	3	4	3	4	3	4	3	4	3.4
2 in Water	0	0	0	0	0	0	0	0	0
(s)-Bupivacaine	4	3	4	4	4	3	4	4	3.8
1d in water	4	5	6	5	5	4	5	6	5.0
1e in water	46	42	44	44	40	48	40	42	43.2

As control group, (s)-Bupivacaine (0.75%, 0.2 mL) can only lead 3.8 h sensory block, which was significantly shorter than data reported by us before (6.0 h).^{S8} This was caused by different standards in these two works on the judgment of sensory block offset. If the standard was changed to that in this work, duration in S8 would be measured to be about 60% compared to reported data.

Neuropathological injury measurement

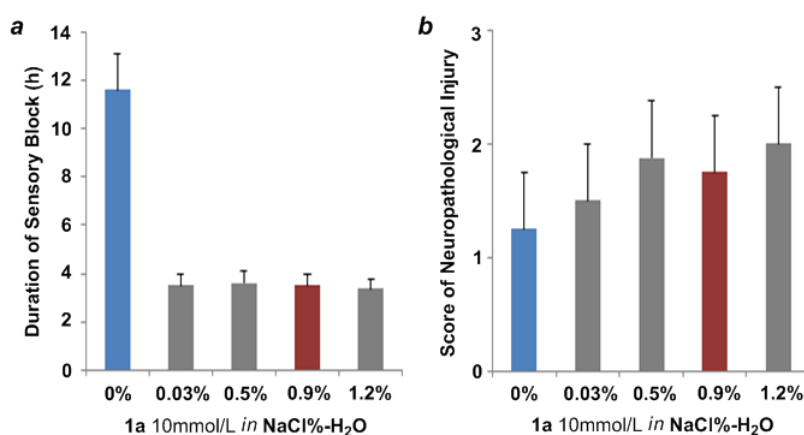
Rats injected by different sample mentioned in Table S8 were killed 7 days after injection. The sciatic nerve was collected and prepared as histopathologic section with HE stain. The neuropathic injury were scored with the same principle of lidocaine salts.^{S9}

The neuropathological injury difference between **1a** in water and in NS was slightly less than our expectation (Table S9). The neuropathological injury scoring of 8 rats injected by **1f** were significantly higher than other groups. These terrible images might be caused by the counter ions of **1f** that were easy to further release H⁺.

Table S9 Neuropathological injury scoring

Injection	Neuropathological Injury Scoring								
	Run 1	Run 2	Run 3	Run 4	Run 5	Run 6	Run 7	Run 8	Mean
1a in water + CO ₂	1	1	0	1	1	1	1	1	0.875
1a in water	1	0	2	1	2	1	1	2	1.25
1a in NS	2	2	1	2	1	3	2	1	1.75
(s)-Bupivacaine	0	1	0	0	1	0	1	0	0.38
1d in water	1	1	0	0	1	1	2	1	1.00
1e in water	1	1	1	2	1	2	1	1	1.25
1f in water	2	3	1	3	3	2	3	2	2.38

The results of rats' sciatic nerve block and neuropathological injury measurement for **1a** in NaCl solution at different concentration were shown in Figure S54.

**Figure S54** Concentration of NaCl scope on rats' sciatic nerve block.

SI.7 Slow release on local tissue measurement

General method on *in vivo* remaining test for 1a on sciatic nerve and muscular tissue:

After intraperitoneal pentobarbital, rats received sciatic nerve block with compound **1a** at 10 mmol/L in water or in NS and bupivacaine at 23 mmol/L. Then each rat was injected with 0.2 ml solution. Tissues of sciatic nerve at injection site with adjacent 1.6 g muscles and connective tissues were harvested. These tissues were washed with pure water to remove the blood residue, crashed, grinded with ice water 0.5 mL and QX-314 as internal standard (0.01 µg) separately in 1min. Each tissue homogenates was added with cool water (25°C water : ice water = 2:1) to make them at the same weight of 4.5 g. The homogenates were centrifuged at 5 °C for 4000 rpm/min during 15 min, and 1.6 g of the supernatant for each group was separately as tested samples. The sample for 0 h was similar with the operation above, and the only difference was that 0.2 ml

solution without injection was added directly into the mixture of crashed tissues and ice water.

The tested samples (3 μ L) were analyzed by LC-MS-MS system by the condition in SI.6. To prevent decomposition, all procedures were conducted at 0°C. Because tested solutions were not completely absorbed in tissues until 0.5 hour after injection, tissue samples were collected at least 0.5 hour after injection to avoid loses of solution. For each test point (0.5, 1, 4, 8, 12, 16 hours after sciatic nerve blockade), n = 6. We defined the average concentration of tissue samples detected by LC-MS at this moment as 100% remaining. The average contents in different time points were then converted into relative percentage of the initial concentration. The *in vivo* release curves of compound **1a** and bupivacaine were thus obtained.

Results

The absolute value of this experiment data cannot be repeated completely by different operators, because the injection sites and muscular tissue samples were difficult to be located accurately, and **1a** was easy to be partly decomposed if the environment temperature increased during the completely operation. Moreover, the primary influence was that the injection at the early time still existed in liquid forms, which was possibly lost during the preparation of muscular samples.

Although the absolute value of this experiment data was not so accurate, we can also make certain that the comparison between **1a** in water and in NS was credible, because all the operations was performed by the same operators at the same time. Thus, it was indicated by the results (Table S10~S13) that **1a** in these different solvents have almost the same slow release behavior in local muscular tissues. That means the duration difference of sensory block was not affected by different slow release manners in local muscular tissues.

Table S10 Local Tissue Remain of **1a** (10 mmol/L) in water + CO₂ after injection

Time Point	Local Issue Remain (ng/mL)						Remain (%)
	Run 1	Run 2	Run 3	Run 4	Run 5	Run 6	
0	4405.27	4225.13	3990.18	4303.52	4044.42	4483.62	100
0.5h	2938.27	3073.25	302.15	3035.36	2922.45	3185.43	71.42
1h	1528.67	1436.25	1508.54	1403.68	1569.25	1397.36	34.75
2h	477.36	621.98	511.63	533.87	582.15	646.27	13.25
4h	154.32	123.25	161.23	222.21	216.73	184.23	4.17
6h	77.35	47.78	58.51	60.32	82.13	69.61	1.55
8h	46.15	40.22	35.43	28.14	34.28	36.22	0.87
16h	17.25	10.47	30.22	9.23	22.54	12.97	0.40

Table S11 Local Tissue Remain of **1a** (10 mmol/L) in water after injection

Time Point	Local Issue Remain (ng/mL)						Remain (%)
	Run 1	Run 2	Run 3	Run 4	Run 5	Run 6	
0	4205.36	4025.89	4215.32	3993.65	3942.18	3983.44	100
0.5h	2579.41	2926.57	2945.72	2508.58	2966.67	2655.34	68.06
1h	1417.47	1370.99	1303.97	1295.28	1158.08	1298.43	32.19
2h	542.86	528.20	399.42	462.61	533.77	495.94	12.16
4h	165.72	131.10	100.70	154.99	102.43	148.55	3.30
6h	48.66	70.78	68.51	60.32	50.13	46.61	1.42
8h	23.42	26.36	37.11	28.96	23.57	29.95	0.70
16h	27.05	12.28	7.64	14.56	9.93	12.24	0.34

Table S12 Local Tissue Remain of **1a** (10 mmol/L) in NS after injection

Time Point	Local Issue Remain (ng/mL)						Remain (%)
	Run 1	Run 2	Run 3	Run 4	Run 5	Run 6	
0	4124.68	4127.52	4133.64	4036.25	4068.3	4110.82	100
0.5h	2420.90	2590.64	2881.90	2383.30	2924.91	3018.23	65.93
1h	1126.76	1060.48	1151.21	1193.22	1095.79	1084.44	27.28
2h	369.74	434.28	400.72	368.94	355.94	420.34	9.55
4h	167.88	100.74	67.95	69.08	131.72	100.74	2.59
6h	75.02	45.68	65.67	58.73	68.92	45.68	1.46
8h	43.92	50.80	47.04	41.18	66.64	43.61	1.19
16h	12.56	36.53	25.60	15.55	6.38	13.84	0.45

Table S12 Local Tissue Remain of (s)-Bupivacaine Hydrochloride (23 mmol/L) in water after injection

Time Point	Local Issue Remain (ng/mL)						Remain (%)
	Run 1	Run 2	Run 3	Run 4	Run 5	Run 6	
0	1332.11	1368.07	1283.26	1422.47	1333.5	1391.01	100
0.5h	502.35	500.21	487.69	532.44	496.33	524.02	37.43
1h	128.21	102.43	140.75	111.29	133.25	101.64	8.83
2h	43.65	38.24	56.75	31.54	25.27	47.23	2.98
4h	1.22	4.07	3.29	4.41	2.78	3.42	0.24

SI.8 *in vitro* diffusion determination on sciatic nerve

18 Sprague Dowley rats (Dossy Experimental Animal Company, Chengdu, China) weighted 200~300g were killed after sedation with inhaled 1.5%~2.0% isoflurane (v/v %) mixing with oxygen. For each rat, two sciatic nerves weighted 1.1g were intercepted rapidly (Figure S55) and stored them in crashed ice separately. 36 sciatic nerves were obtained, and 30 of them with approximate thickness were selected for the next step. Sciatic nerves bifurcated was abandoned.

All of these 30 sciatic nerves were washed with pure water to remove the blood residue, dried by filter paper and cut into 1.10 g intact standard samples. These standard samples were put into 30 glass bottles individually with **1a** solution (10mmol/L) at 40 °C approximate to the internal temperature of rats for 0.5 hour. Then these 30 samples was removed from the **1a** solution, washed with pure water, dried by filter paper, crashed, grinded with ice water 0.5 mL and added with QX-314 as internal standard (0.01 μ g) separately in 1min. Each tissue homogenates was added with cool water (25°C water : ice water = 2:1) to make them at the same weight of 2.0 g. The homogenates were centrifuged at 5°C for 4000 rpm/min during 15 min, and 1.6 g of the supernatant for each group was separately as tested samples.

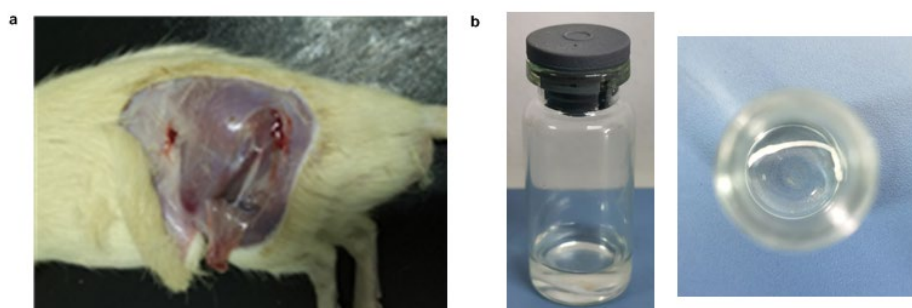


Figure S55 a) Images of rat's sciatic nerve **b)** Images of rat's sciatic nerve 0.5 h after diffusing into solution

Results

The results were shown in Table S13. Values of Average (%) were compared to **1a**, **1d** and **1e** with different molecular weight separately.

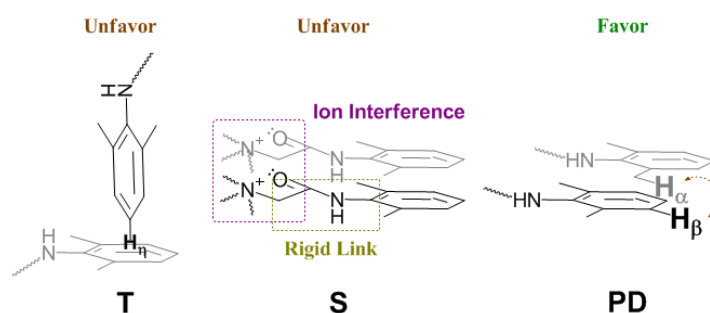
Table S13 Local tissue contain in sciatic nerve *in vitro*

Sample	Local Issue Contain (ng/mL)						Average (%)
	Run 1	Run 2	Run 3	Run 4	Run 5	Run 6	
1a in water + CO ₂	345.23	337.36	351.39	341.08	390.21	406.11	39.59
1a in water	399.25	412.32	365.23	391.25	387.86	433.41	43.56
1a in NS	732.60	668.14	725.33	692.69	780.36	757.38	79.43
1d in water	322.54	408.71	353.05	352.02	433.83	377.06	36.24
1e in water	349.34	385.76	345.42	286.13	395.15	280.82	36.25

SI.9 Data summary

pKa of HX is used to describe the acid strength of X in inorganic chemistry. Smaller pKa of HX for compounds with same cationic structure and different counter ions of X represent tighter ion pairs, which leads the whole compound more difficult to achieve ion-exchange for other anions in liquid environment.

1a, **1d** and **1e** have same organic structure on cationic part of molecules. Nano systems self-assembled by these molecules were proved to be arranged in similar manners based on parallel-displaced π - π stacking by the correlation signal of H_α - H_β mentioned above. It was difficult for these molecules change their arranged manner into T-shaped or parallel-sandwich structure. T-shaped structure was absolutely different from parallel-displaced π - π stacking, so that molecules were considered to be difficult to coexist in these two manners. These molecules were suspected to be difficult to exist in parallel-sandwich π - π stacking due to ion interference between cationic head and carbonyl group in different molecules, as shown in Scheme S8. Amide group rigidly connected between cationic head and aromatic ring would enhance the intermolecular ion interference. Parallel-displaced π - π stacking was confirmed to be favored model than the other two models. Peak areas of H_α - H_β for nano systems self-assembled by these three compounds, are thus used to represent proportion of π - π stacking in intermolecular ^1H - ^1H NOESY test in same condition. Larger peak areas of H_α - H_β indicated higher proportion of π - π stacking



Scheme S8 Parallel-displaced π - π stacking is favored on supramolecular arrangement of **1a**, **1b**, **1d** and **1e**.

Table S14 Summary of sensory block duration, CMC, pKa and π - π stacking

Sample	CMC (mmol/L)	Particle	pKa of HX	Area of H_α - H_β	Sensory Block Duration (h)	Neuropathological Injury Scoring
1a + CO ₂	15.33	SMs	-8.0	6.90	12.1	0.875
1a	16.16	JPs + SMs	-8.0	61.99	11.6	1.25
1a in NS	2.83	SMs-like	-8.0	811.17	3.4	1.75
1d	11.70	SMs + SMs-like	-1.9	57.06	5.0	1.00
1e	7.10	Vesicles + SMs	-3.0, 1.99	175.08	43.2	1.25

Data of rats' sensory block duration, CMC of nano systems, pKa of HX and peak area of H_α - H_β are summarized in Table S14. CMC seems to be irrelevant to block duration. pKa and π - π stacking

are considered to be of importance on the stability of nano particles, which were related to their behaviors of self-delivery and self-release *in vivo* to affect efficacy of sensory block (Scheme 4).

References

- [S1] Tang, L.; Yang, J.; Yin, Q. et al. *Chem. Commun.* **2017**, 53, 8675–8678.
- [S2] Feng, D.; Zhang, Y.; Chen, Q.; Wang, J.; Li, B. Feng, Y. *J. Surfact. Deterg.* **2012**, 15, 657–661.
- [S3] Dixon, W. J. *Neurosci. Biobehav. Rev.* **1991**, 15, 47–50.
- [S4] L. Tang, F. Qin, D. Gong et al. *Chem. Commun.* **2023**, 59, 1653–1656.
- [S5] Liu, J.; Ke, B.; Zhang, W. and Yang, J. CN112574098A.
- [S6] Liu, J.M.; Lv, X. *Int. J. Mol. Sci.* **2014**, 15, 17469–17477.
- [S7] Binshtok, A.M.; Gerner P.; Bae, S. *Anesthesiology* **2009**, 111, 127–137.
- [S8] Liu, J.; Tang, L.; Zhang, W. et al. CN 110092731A.
- [S9] Thahammer, J.R.; Vladimirova, M.; Bershadsky, B.; Strchartz, G.R. *Anesthesiology* **1995**, 82, 1013–1025.